Adhesion force measurement of the solid-liquid interface

by

Palak Jain

A thesis submitted in partial fulfillment of the requirements for the degree of

Master of Science

Department of Mechanical Engineering
University of Alberta

Abstract

Wetting is the process where solid surfaces attempt to create a common interface when they come in contact with the liquid droplets. To characterize the wetting and spreading between a liquid droplet and a solid surface, various techniques have been established. The most common technique have been used past over two decades is the measurement of contact angle, defined as the angle formed at the interface where all three phases (solid, liquid, surrounding medium) meet. Although contact angle measurements have been studied for over 200 years, the authentic procedure or guidelines to measure contact angle is still in debate. Some authors prefer to quantify surface wettability using dynamic contact angles, whereas some authors report static contact angles measured between a liquid drop sitting on a solid surface. This study discusses the alternative and reliable method for quantification of wettability and adhesion, *i.e,* adhesion force-based measurements using a micro-electronic mechanical balance system. In this technique, a drop holder is suspended and a liquid drop of the desired volume is generated at the tip of the holder facing toward the characterizing substrate. A series of commands has been initialized such as interaction and formation of solid-liquid interface, compression, retraction, and drop detachment, while continuously recording the interactive vertical forces, experienced by the force sensor. There are various parameters/variables involved in this study, which resulted in the variation of droplet base diameter and eventually affect adhesion force. These parameters such as drop volume, retracting speed, and compression allow to maneuver the adhesion force to obtain the required adherence or attachment between two surfaces. After es-

tablishing the guidelines to record reproducible and repeatable (R & R) results and studying the effect of these commonly operating parameters on adhesion force, we have also discussed the effect of the surrounding medium and performed experiments in the liquid medium. Unlike the air medium, we observed that the force sensor experienced other forces as well along with interactive forces underwater. Forces such as buoyancy and hydrostatic pressure must be subtracted from total vertical force to get absolute adhesion force. Lastly, components of adhesion force; surface tension, and Laplace pressure force are also critically analyzed with respect to drop volume and compression. This study also introduces the normalization of total adhesion force and its components to negate the influence of varied droplet base diameter.

Preface

The work in this thesis is original work by Palak Jain, supervised by Dr. Prashant R Waghmare. I was responsible for the experimental design, conducting experiments, data interpretation, developing the theoretical framework and analysis, and manuscripts. The idea for this project was conceived by my supervisor who was involved with the conceptualization and editing of the manuscripts. The interpretation of data was performed by myself with valuable discussions with my supervisor. Dr. Aleksey Baldygin, Dr. Thomas Willers, and Dr. Butunath Majhy contributed to reviewing the manuscripts to their best ability.

A version of Chapter 3 of this thesis will be submitted to Nature Protocol as: Palak Jain, Aleksey Baldygin, Thomas Willers and Prashant R. Waghmare, "Adhesion force quantification for a solid-liquid interface".

Furthermore, a version of Chapter 4 will be submitted to the Journal of Soft Matter with authorship order as: Palak Jain, Butunath Majhy, Aleksey Baldygin and Prashant R Waghmare, "Study of adhesion force in different operating parameters and surrounding medium".

Part of this thesis work has also been presented (virtually) in Droplets Conference 2021 (Droplets 2021), Darmstadt, Germany, August 16 - 18, 2021, and (in person) in American Physics Society (APS March Meeting), Chicago, US, March 14 - 18, 2022.

Acknowledgements

Table of Contents

List of Tables

List of Figures

Chapter 1

Introduction

Studies of surface wettability have always been an essential branch of science due to its existence in almost all facets of our daily activities such as cleaning, cooking, washing, shaving, and so on. Therefore, mastering and controlling solid-liquid interactions have become crucial and critical in many industries such as anti-biofouling coatings [1], anti-corrosion [2], self-dirt removal surfaces [3, 4], oil-water separation [5], to name few [6–9]. Additionally, phenomena found in nature known as the lotus effect, the ability of a surface to roll-off water droplet [10], gecko feet for reversible adhesion, and many more [11–13] inspired researchers to replicate and fabricate superhydrophobic and self-cleaning surfaces [8]. Fundamental understanding of such interactions in terms of spreading and adhesion has been investigated by many researchers and several revolutionized conclusions have been established [14, 15]. The very first mathematical relation found was written by a famous scientist, Dupre in 1869 [16], called Young's equation, which is also known as the Young-Dupre equation. The equation defines the contact angle (CA), which is the angle between the solid surface and the tangent to the liquid-medium interface plotted at the point of contact between three phases. It is related to the surface energies per unit area of the solid-liquid, solid-vapour, and liquid-vapour, γ_{SL}, γ_{SG}, γ_L, respectively [17] (see Figure 1.1).

$$cos\theta_Y = \frac{\gamma_{SV} - \gamma_{SL}}{\gamma_{LV}} \tag{1.1}$$
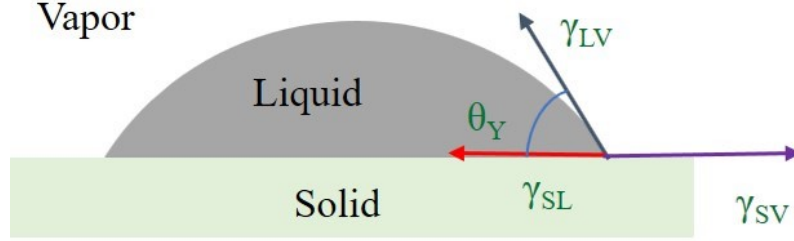
Figure 1.1: A drop of water is sitting on an ideal solid substrate.

θ_Y, is also known as equilibrium contact angle or ideal contact angle.

Moreover, surfaces with CAs ranging between 10°- 90° are called hydrophilic surfaces, whereas surfaces with higher contact angles ranging between 90°- 120°, are termed hydrophobic surfaces [18]. For above 120°, surfaces are called superhydrophobic with CA between 150° - 160° showing high repellency to water such as lotus leaves [19].

However, Young's equation is only valid for smooth, non-deformable, homogeneous, and rigid surfaces, which rarely exist in real-based applications [20]. Later, Wenzel equation [21], Cassie equation [22], Cassie-Wenzel equation [23], and Cassie-Baxter equation [24] were developed, which take into account a surface roughness, smooth heterogeneous surfaces, rough heterogeneous surfaces, and surfaces with air pockets that are not penetrated by the wetting liquid respectively. Although various models have been proposed for surfaces with different topographical and chemical heterogeneities, none of the above-mentioned equations clarify the droplet pinning effect or hysteresis effect at the three-phase contact line (TPCL), which can be induced due to different compositions at various local regions [25–28].

Furthermore, due to the common practice of the these equations, and not addressing above mentioned limitations, it has led to the rise of another issue or debate in the literature, *i.e,* frequent use of "static" term to define contact angle of a liquid drop sitting on the surface [23, 30]. This approach assumes that it is Young's equilibrium contact angle or ideal contact angle with global energy minimum, which interprets
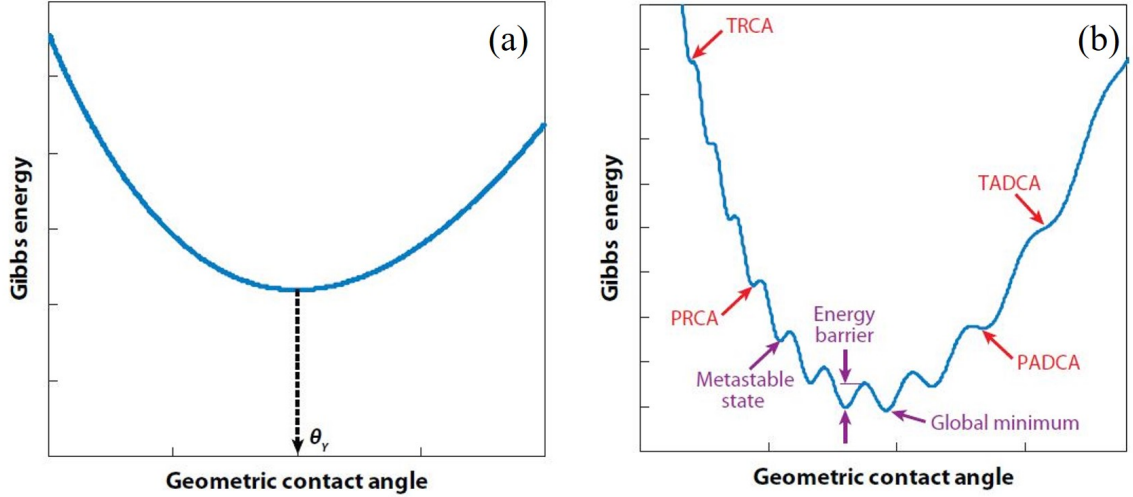
Figure 1.2: The Gibbs energy versus the contact angle on (a) ideal surface (b) on heterogeneous surface. Each minimum represents a metastable equilibrium state. There exists an energy barrier in between every pair of equilibrium states. Abbreviations used: PADCA, practical advancing contact angle; PRCA, practical receding contact angle; TADCA, theoretical advancing contact angle, TRCA, theoretical receding contact angle [29].

thermodynamically that there is only one minimum value on the Gibbs energy curve i.e., Young CA (see Figure1.2 (a)), represents equilibrium state on an ideal surface [31, 32]. However, due to heterogeneous surfaces as a consequence of surface roughness or different chemical compositions, there exist more than one local apparent CAs [33–36]. These local CAs at various locations might be equal to local Young CA, which implies that this could be at the equilibrium state system. These states are termed metastable, associated with a local minimum in Gibbs energy. The critical judgment here, is these local apparent CA values are different for each such state, and the lowest of all Gibbs energy values define the most stable state as shown in Figure 1.2 (b). Marmur [29, 37] explained that the "static" contact angle reported in the literature between a solid-liquid interface could be in any local energy minimum, and instead of being most stable CA, it could be metastable CA. From this curve, we can also define the dynamic contact angles, which are the highest CA in this range, termed advancing CA and the lowest CA in this range would be receding contact an-

3

gle. To streamline, the measurement of these static contact angles is not repeatable or reproducible, which brings the conflict in reporting values in the articles for the same solid-liquid interface. Recently, in 2019, Huhtamaki *et al.* [38] presented guidelines to produce repeatable and reproducible advancing (ACA) and receding (RCA) contact angles using a goniometer and increase/decrease drop volume of a sessile drop, by considering substrates of different surface topographies and wettability.

To summarize, wettability measurements are important to characterize solid-liquid interaction. Therefore, for the constructive and quantitative conclusions, there are further proposed methods such as dynamic contact angle measurements, contact angle hysteresis, and in some cases the surface energy quantitation and (solid-liquid interface) adhesion force measurements. Here, we focused on adhesion force measurements using a micro-electronic mechanical balance system and the detailed scrutiny of different operating parameters that affect the adhesion force measurements.

1.1 Why Adhesion force measurement is important

Although significant studies have been reported on the contact angle measurements in the literature, the correlation between the contact angle to the surface wettability and adhesion has not received the due credit and importance in the literature [39, 40]. The fundamental question remained to be answered, how are these surface properties correlated to the interactive forces between liquid droplet and solid surface? Law et al. [41], Butt et al. [42, 43], and Jiang et al. [44] and Amirfazli et. al. [45] have studied several surfaces and attempted to correlate the wettability and adhesion force. They concluded that force at the onset of the drop formation (called as snap-in force) and at the force at the instant of drop detachment (called as pull-off force) are related to advancing and receding CAs, respectively. Apart from such studies no literature aimed to relate the adhesion force and wettability, in particular
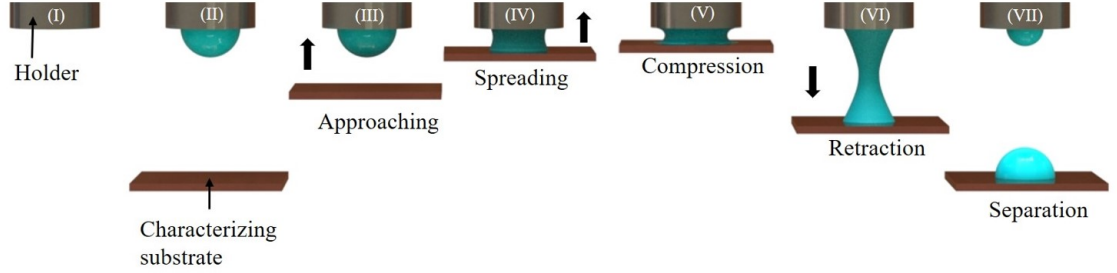
Figure 1.3: Schematic of the steps involved to measure adhesion force.

the nuances of different operating parameters on the measurements. Through these studies [41–45] it was clearly articulated that the adhesion force measurements are the appropriate representation of the solid-liquid interaction rather than a localized CA measurements. Therefore, in the next section, the details of the adhesion force measurement is examined.

Figure 1.3 shows the schematic representation of the process involved in measuring adhesion force, using a force tensiometer or a microbalance. Firstly, the holder is connected to the force sensor, followed by the deposition of a liquid droplet onto it and placing the characterizing substrate on a moving stage vertically − aligned with gravity. The characterizing substrate starts approaching the liquid droplet until the solid-liquid interface forms. After detecting the solid surface (sudden change in force experienced by balance), compression of a fixed distance is achieved for uniform spreading. Followed by, retraction of the characterizing substrate. Before the retraction starts, different theory and users suggests the important of residence time and compression for the formation of equilibrium TPCL. The importance of such operating parameters and appropriate selection of these parameters significantly alters the final measurements. Therefore, we have devoted the entire Chapter 3 to establish the protocol of adhesion force measurements. After the formation of the TPCL, the retraction of the substrate begins resulting into the elongation of liquid profile and eventually breaking up of the liquid bridge between the holder and the substrate. The retention volume on either side depend on numerous parameters that we will

elaborate in subsequent Chapters 3 and 4.

Here, from a theoretical standpoint, as presented in Equation 1.2, the adhesion force, measured by the instrument consists of two components: (i) surface tension force, the force at the three-phase contact line (TPCL) and (ii) the Laplace pressure force, $\triangle$ P acting across the interface.

:

$$F = 2\pi r\gamma \, sin\theta - \pi r^2 \triangle P \qquad (1.2)$$

where θ is the instantaneous contact angle (measured at corresponding instantaneous interactive force), r is the droplet base radius, γ is the surface tension of the liquid in air medium, and $\triangle$ P is the Laplace pressure.

In Chapter 4, we have studied the Laplace pressure force and surface tension force components separately with the variation of TPCL and discussed the importance of contribution of each component to the total adhesion force measured experimentally.

1.2 Overview of applications

The wetting and adhesion characteristics of a liquid droplet sitting on a solid surface, either flat or textured, homogeneous or heterogeneous cover a wide range of applications [46–48]. Due to advances in techniques and processes, now it's able to replicate nature-inspired liquid-repellent surfaces, for a variety of applications such as drag reduction [4, 19], anti-icing surfaces [49], oil-water separation [50], self dirt removal [15, 51], and droplet microfluidic devices [52]. Meihua Jin et al. [53] characterized surface wettability using adhesion force-based measurements in 2005. They have developed superhydrophobic polystyrene (PS) layer due to its great interest in practical applications such as hotspot cooling, anti-corrosion, anti-reflecting coatings, spray painting, and anti-bacteria to name a few [1, 3, 54–59]. In addition, Samual et al. [41] studied the correlation between the measured adhesion force using a force tensiometer and surface properties using a goniometer for electrophotographic print-

ing applications [60–62]. This study was achieved to understand surface wettability using adhesion force measurements and optimize the liquid transfer between two surfaces for better image integrity and resolution control in printers [63]. In addition, the adhesion strength between solid-liquid interaction determines the stability of liquid film between the gas bubble and the particle surface [64]. Numerous industrial processes such as wet processing of materials, wastepaper deinking, sewage treatment technologies, enhanced oil recovery, and many others, benefit from understanding the wetting characteristics of solid surfaces [65–70].

Similarly, solid-liquid interaction is of great interest to fundamental research and industrial applications for the liquid medium as well. For instance, underwater submerged superoleophobic materials have shown encouraging advantages in resolving the incessant oil slick mishaps [71]. Frequently, appeared oil leaking and heavy emission of various oily water have caused a serious threat to water living bodies and the environment [72, 73]. It is essential to prevent waste oil from further migrating. Therefore, among other methods, it is highly desirable the development of novel superoleophobic surfaces. These surfaces/materials have the exceptional oil-repellency characteristics to enable only water to permeate through them. In addition, recent progress in underwater superoleophobicity has opened a new approach for the utilization of innovative membrane materials for rapid and effective separation of oil/water mixtures, which has increased interest from researchers [74–76]. Henceforth, such materials turn out to be profoundly attractive to create eco-accommodating and proficient results.

These super-anti wetting surfaces have drawn significant consideration because of their incredible benefits in industrial applications such as preventing blockage, bio-adhesion, microfluidic technology, and oil water-separation [77–80]. Inspired by many natural biological surfaces, such as fish scales [81] and nacre's shell [82], authors have also focused on the structure-dependent controllable underwater oil adhesion [83].

Although there are numerous studies to fabricate these super-anti wetting surfaces for air and liquid medium, the characterization of such surfaces is still challenging. Investigation of surface properties of these surfaces are highly-dependent on contact angle based measurements. As we know, point of contact is minimum in superhydrophobic and superoleophobic surfaces, it is critical to define contact baseline using optical setup. This may results into inaccurate data and loss of important key results. Therefore, adhesion force measurements are the most suitable performance indicator which entirely based on the force experienced by the force sensor during solid-liquid interaction.

1.3   Problem statement

Although adhesion force measurements using a force tensiometer is the new rising technique to characterize the wetting properties, due to its accuracy and precision, the details of the method are still not explored yet.

- For instance, there is no attention given to the role of the holder used, to suspend the liquid droplet. There is literally no significant discussion yet in the literature about the material properties, the shape, and configuration of drop holder [41, 173].

- Second, due to the accessibility of only one i.e. ring based shaped holder, the study of any solid surface, be it smooth or chemically or physically modified surfaces is restricted to the utilization of a single drop volume value. That means it is difficult to study the influence of drop volume on adhesion force, measured using a micro-electronic mechanical balance system [53].

- Moreover, in the process of measuring adhesion force, other than drop volume, there are other parameters such as the compression, retracting speed, time

period provided to form the interface equilibration, which are not discussed in detail [68].

- In addition, literature discusses adhesion force-distance curve for underwater studies for a given solid-liquid interface. However, it is observed that some negative forces are experienced by the force sensor before even the solid liquid interacts, which haven't been addressed yet so far. To have a better assessment of adhesion force in the liquid medium, it is important to consider external forces, other than interactive force, to gain a complete understanding of absolute adhesion force measurement [163].

- Furthermore, from a theoretical standpoint, total vertical adhesion force consists of surface tension and Laplace tension force as discussed in section 1.2, it is observed that the surface tension force is the major dominating force [84]. However, the significance and contribution of Laplace pressure to total adhesion force have not been critically analyzed so far in the literature. Therefore, it is also important to analyze both the components individually to understand their behavior with respect to varying operating parameters [84].

1.4   Aim of present work

Considering all these above mentioned aspects, this project presents:

- A detailed procedure to accurately and repeatedly record adhesion force, using a force tensiometer between a liquid droplet and a solid surface.

- Provides guidelines to take consideration of additional forces in liquid media such as buoyancy and to calculate absolute adhesion forces in liquid medium.

- The influence of operating parameters like drop volume, magnitude of compression and surrounding medium on maximum adhesion force is also considered.

- Later, components of adhesion force were studied individually to negate the influence of these operating parameters.

1.5   Thesis outline

The main objective of this thesis is to provide the accurate guidelines to record the adhesion force between a liquid droplet and a solid substrate in both, air and liquid mediums. Hence, in this section, we described the structure of the thesis, basically topics covered in the succeeding chapters.

Chapter 2 is the review of the literature for force-distance curves and adhesion force. In this chapter, we have discussed the origin of the measurement of interactive forces. For instance, B.V. Derjaguin and Abricossova were the first in the 1950s to perform the direct measurement of molecular attraction between solids separated by a narrow gap. Inspired, Tabor and Winterton also recorded surface forces using an optical interference technique in 1969. These findings lead to the introduction of the Surface Force Apparatus (SFA) in the 1970s. Later, we also covered the brief introduction and applications of Atomic Force Microscopy (AFM) and Scanning Tunneling Microscope (STM). After discussing the history of the force-distance curve, the evolution of AFM from the 1980s to the 20s was briefly covered. It is observed that the AFM technique is widely used for surface characterization and surface mapping, and to identify the surface wettability and adhesion force. Later, we concluded the chapter by comparing and discussing other measurement methods to measure solid-liquid interaction based on end-user applications. Finally, we summarized the need to study the adhesion force measurements using a force tensiometer to provide accurate and correct key results.

In Chapter 3, a detailed protocol (series of steps) for measuring the total interactive and other forces (in air and liquid medium), experienced by the force sensor is given. Firstly, different drop techniques were investigated, where drop is gener-

ated at different holders of varying material and configuration properties. This study is achieved to select the best-suited drop holder to suspend the liquid droplet, preventing any hindrance or limitations to droplet spreading. This chapter also gives insight into guidelines on camera settings, such as frame rate, magnification, focus, and calibration, which facilitates the optical method to be more synchronized and precise while capturing the phenomenon. This chapter includes complete and a detailed procedure such as pre-measurement, measurement, and post-measurement of the adhesion force-distance-time curve. In post-measurement, we discussed the exporting and plotting of the adhesion force curve and the necessary steps to take to calculate absolute adhesion force in the liquid medium. In addition, the data analyses for images/videos are also covered to measure droplet base diameter, contact angle, and user-required other parameters.

In Chapter 4, after considering and discussing the guidelines to record the adhesion force for a given solid-liquid interface, in a given fluid medium. The the role of different operating parameters such as drop volume and magnitude of compression has been analyzed. Role of the droplet holder is already covered in Chapter 3. The adhesion force-distance curve is obtained for water droplets, interacts with Poly(methyacyrlate), Teflon, and Polyamide (PA) in air medium and for silicone oil (D10) with Poly(methyacyrlate), Teflon, and Copper in liquid medium. For liquid media study, water is used as the surrounding medium because of several underwater applications, already covered in section 1.3. The direct relation of these parameters on maximum adhesion force (F_{max}) has been studied. Furthermore, to gain understanding about components of adhesion force, *i.e.,* surface tension and Laplace pressure force, the role of these parameters (drop volume and compression) has also been investigated on them individually.

Finally, the last chapter (Chapter 5) presents a brief conclusion and discussion about the entire thesis work and the potential future topics, respectively. The re-

sults obtained from the previous chapters have given the insights into accurately and precisely measuring adhesion force using a force tensiometer, that can be applied to characterize the surface properties of altered or unaltered solid surfaces.

Chapter 2

Literature Review

In order to account for intermolecular forces between the finite sizes of molecules, J.D. van der Waals introduced two correction terms to his perfect gas equation in 1873 [85, 86]. Between atoms and non-polar molecules, the van der Waals (vdW) forces are always attractive. They are crucial for adhesion as well as the stability of colloids and foams [87, 88]. They also play an important role to determine the viscosity and surface tension of liquids as well as some of the strength properties of solids. The most direct way to study these forces is to measure the surface or attractive forces between two solid surfaces separated by a distance gap as a function of their separation [89, 90]. Measurement of surface forces between two solid surfaces separated by a gap width is experimentally challenging [91, 92]. Direct methods using model surfaces are made difficult by the short range and the small magnitude of the force. The instrumentation and methods of measuring surface forces are various and numerous [93, 94]. In this chapter, we have discussed different techniques which involve the measurement of surface force as a function of the separation or the distance between two surfaces as shown in 2.1. This literature review covers a brief discussion and the history of the direct measurements of surface forces by studying the measurement of vdW forces between two surfaces in the early 1900s and followed by the invention of Surface Force Apparatus (SFAs). Then, we covered the limitations of the Surface Force Apparatus and discussed the invention of Atomic Force Microscopy (AFM)
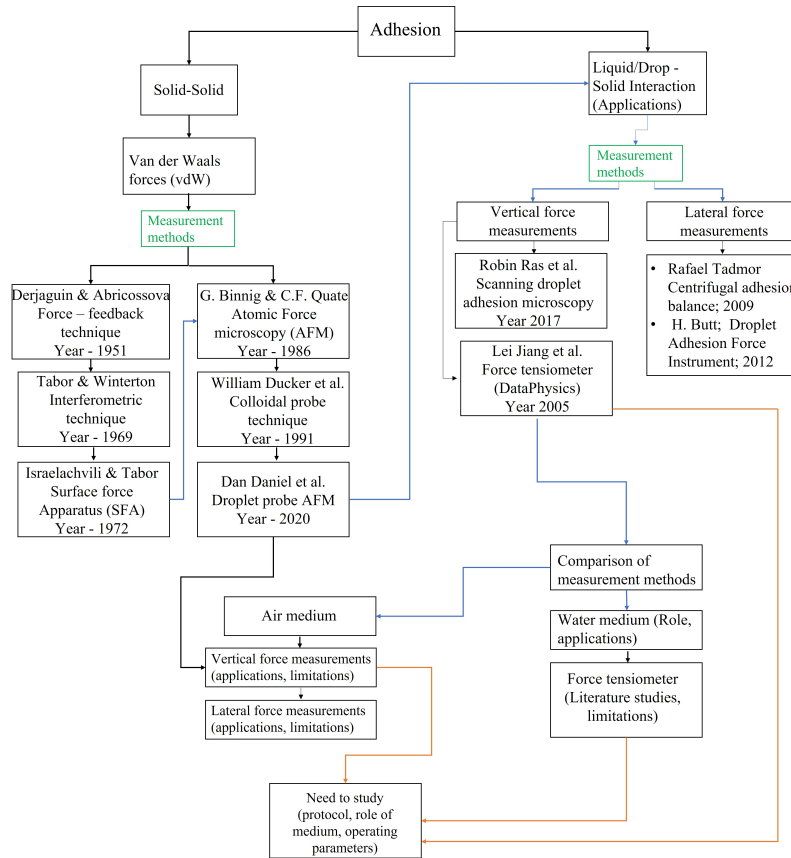
Figure 2.1: Flow chart representation of the literature review. Here, blue, black and orange arrows indicates the flow of the chapter, classification and motivation, respectively.

in the later section. Conclusively, the employment of AFM benefited the material science community to characterize chemically and physically modified surfaces has been considered. This brings us to the discussion of the wetting phenomenon and liquid droplets' interaction with solid surfaces. To better understand the solid-liquid adhesion, we also have studied other measurement techniques to record the force-distance curve between a liquid droplet and a solid surface in a given surrounding fluid medium.

2.1 Solid-solid adhesion

The first accurate measurement of vdW forces was performed by Derjaguin and Abricossova in 1954 [95, 96] using the ingenious force-feedback technique. They have developed the first non-interferometric method to measure the interactive forces between smooth transparent solid substances. In the measurement, a beam-type microbalance with photoelectromagnetic negative output has been employed to record both attractive and repulsive forces. The distance between the surfaces was controlled by rotating an elastic torsion suspension relative to the fixed surface [88, 97]. The molecular attraction between two quartz glass has been detected with the measured forces in the range from 1-2 x 10^{-4} to 20 dynes with the gap widths from 10^{-5} to 10^{-3} cm [98].

Followed by this work, in 1969, D. Tabor et al. [90, 99], considered the interferometric method using fringes of equal chromatic order (FECO) to measure van der Waals forces. Their results provided a direct measurement of the magnitude of these forces between mica sheets separated by a distance gap between 5 to 30 nm in air [100, 101]. In the experiment two thin mica specimens were bent into a cylindrical shape with their axis mutually at right angles as shown in Figure 2.2. To determine the force, the lower specimen was held fixed and the upper specimen was held at the end of an elastic beam (see Figure 2.2). Here, one specimen moved towards the other using a piezoelectric transducer. At a critical separation, the surface jumps to contact. This happens when the attractive forces between the surfaces overcome the stiffness of the spring [102, 103]. They were able to vary the stiffness of the elastic beams to analyze the jump at different separation distances.

Later in 1972, J.N. Israelachvili and D. Tabor [104, 105] worked on the measurement of vdW dispersion forces for separation distance in the range of 1.5 - 130 nm. This leads to the invention of the surface force measuring technique in 1976 called Surface Force Apparatus (SFA) using the interferometric technique. Later this in-
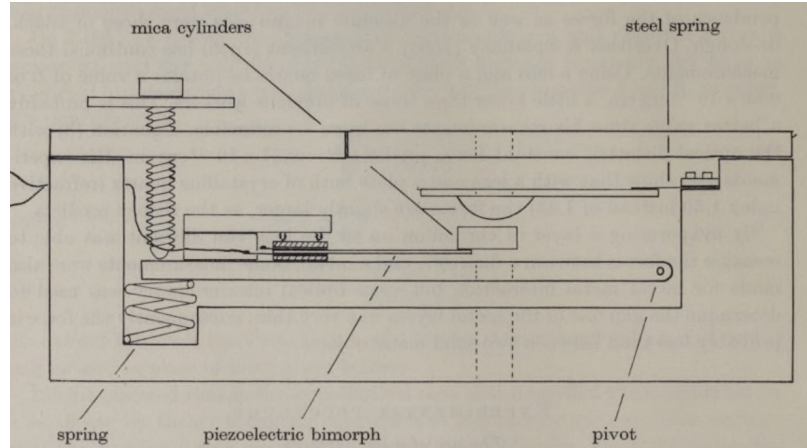
Figure 2.2: The experimental apparatus designed by Tabor and Winterton for measuring vdW forces between two smooth mica sheets [90].

strument was refined by Israelachvili and Adams and known as SFA Mk I [106, 107]. SFA has the ability to measure forces for a separation distance within 0.1 nm. The instrument enabled the first detailed measurements to be made of the two fundamental forces of colloid science. These are the repulsive electrostatic double-layer forces and the attractive vdW, which exist between any two charged surfaces immersed in an electrolyte solution [108, 109]. The apparatus was constructed to measure the forces between surfaces in liquids and vapors [110]. These forces were measured by two different methods based on the range of gap width: (1) is the jump method which is in the range of 1.5 to 20 nm, and (2) the resonance method, in the range of 10 to 130 nm. Later in 1985, Israelachvili measured the static and dynamic interactions of very thin liquid films between two surfaces as they are moved normally or laterally relative to each other [111, 112]. The main challenge with this instrument was always in the design of a mechanical device in order to successfully incorporate at the angstrom level. In addition, Mk II was introduced to accommodate all the issues and concerns with Mk I, such as the the replacement of the single-cantilever force-measuring spring by a variable-stiffness double-cantilever spring which extended the range of measured forces [112]. Finally, Mk III was also developed with much more stability and accessibility to clean and operate easily.
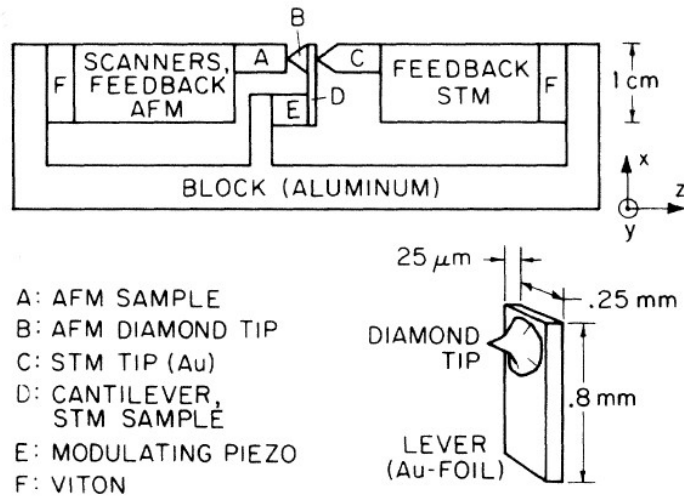
Figure 2.3: Experimental setup of AFM [113]

2.2 Introduction to Atomic Force Microscopy

After discussing the interferometric methods to directly measure the surface forces, another technique was also proposed to study the surface profile at nanometer scale. G. Binnig et. al. [113, 114], invented one of the series of scanning probe microscope, named as Atomic force microscopy (AFM) in 1985 at the IBM Zurich Research Laboratory. In his work, AFM is reported as a combination of the principles of the scanning tunneling microscope and the stylus profilometer. In the experimental setup as shown in Figure 2.3, the sample is scanned by a tip, which is mounted to a cantilever spring. The force between the tip and the sample is measured by monitoring the deflection of the cantilever, while scanning. It provides the topographic image of the sample by plotting the deflection of the cantilever versus its position on the sample [115–117].

After the invention of AFM for imaging the topography of surfaces with high resolution, it is realized that it can be used for force-verses-distance measurements as well [118, 119]. These measurements were further investigated to study properties of the sample. In AFM force measurement, the tip attached to a cantilever spring is moved towards the sample in normal direction. Vertical position of the tip and
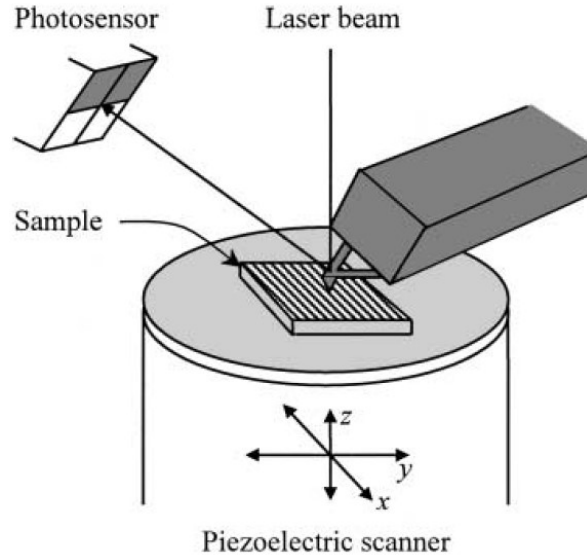
Figure 2.4: Experimental setup of colloidal probe technique [113].

deflection of the cantilever are recorded and converted to force versus distance curves. Later in 1991, Ducker et al. [120], replaced the tip by a colloidal particle of known spherical radius and this technique is termed as colloidal probe technique. This technique is widely used in recording the particle interaction with the surface and measuring the surface forces with separation for a variety of different applications [118].

In the experimental setup of the colloidal probe technique or AFM, as shown in Figure 2.4, A piezoelectric scanner is employed where the sample is mounted for its fast and high precision motion by applying voltage. A laser beam is focused onto the back side of the cantilever and the deflection of the cantilever is captured by a sensitive detector. Later the data collected from the detector signal in volts and the piezoelectric translator are converted to force and displacement results respectively. Figure 2.5 represents two graphs, one (a) is plotted with deflection signal versus piezo position and the other (b) Corresponding force versus distance curve.

Since, its invention, AFM has been used for a variety of operation modes such as surface characterization at the atomic scale, measuring surface forces, to map the

18
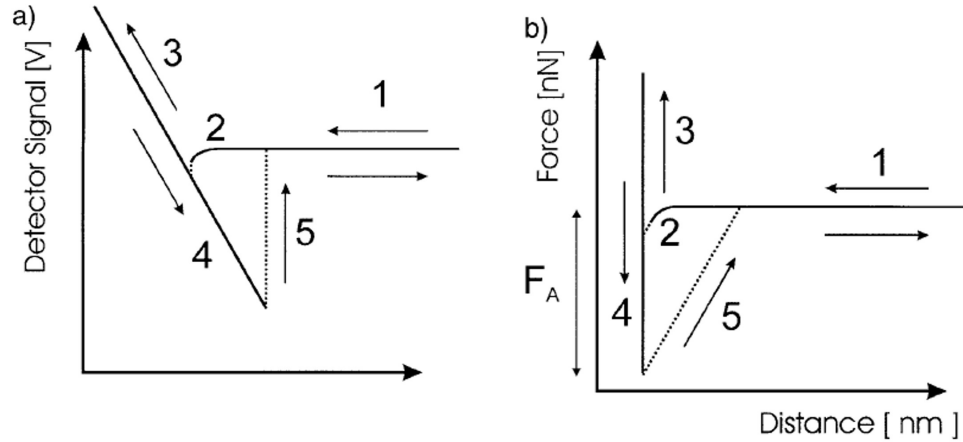
Figure 2.5: (a) Schematic of a deflection signal versus piezo position curve. (b) Corresponding force versus distance curve after multiplying the deflection with the calibration coefficient obtained from a linear fit of the constant compliance region and the spring constant of the cantilever, and adding the cantilever deflection to the piezo position. F_A denotes the adhesion force [118].

surface topography of altered surfaces due to its high lateral resolution at atomic scale [121, 122]. Furthermore, AFM opens the possibility to image liquid structures on the nanometer scale. This study determines the liquid-tension of a solid-liquid vapor TPCL and studied the drop size dependency on the contact angle using AFM and compared with conventional techniques of optical contact angle goniometry [123, 124]. This brings us to the important topic in the science community of wetting phenomenon due to its numerous industrial-based applications [125]. As we already know from Chapter 1 the significance of surface wettability and surface adhesion in nature and in industrial-based applications. We have briefly studied other measurement methods in the literature to measure solid-liquid interaction in the next section.
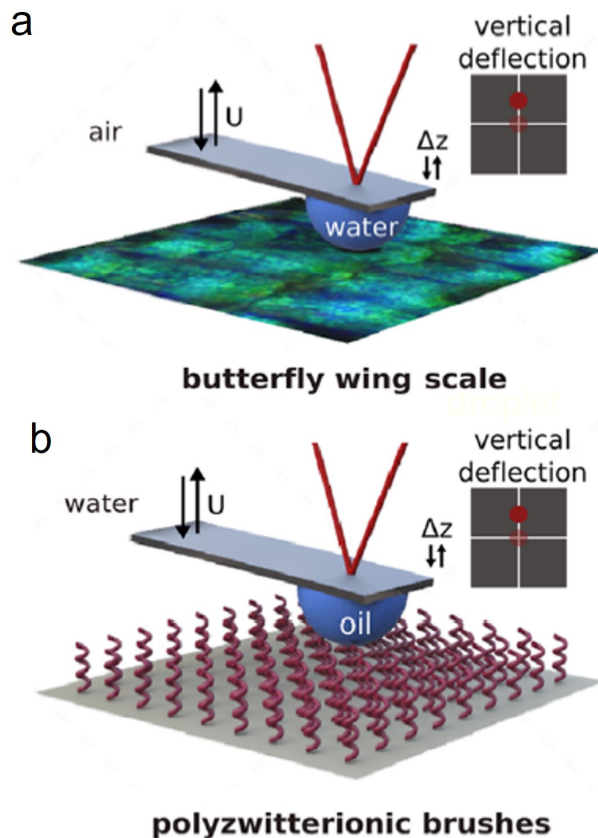
Figure 2.6: Schematic illustration of the water and oil droplets in contact with (a) butterfly wing scales and, (b) zwitterionic pSBMA brush surface (under water), respectively [126].

2.3 Different methods of measuring solid-liquid interaction

2.3.1 Vertical force measurements (Normal to TPCL)

The term vertical or normal force measurements is implied when the liquid droplet and solid surface are brought in contact with each other through vertical motion (the axis of travel is inline with gravitation acceleration) and performed series of steps. AFM is one of the vertical force measurements techniques used to record force-distance curve. Here, we have discussed the droplet probe AFM method to characterize solid surfaces.
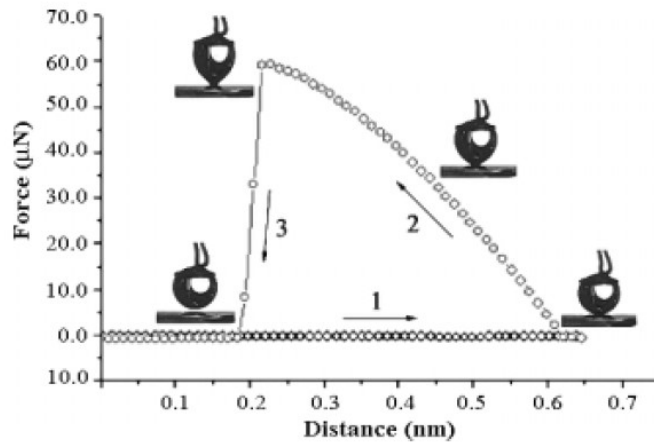
Figure 2.7: Force-distance curves recorded before and after the water droplet makes contact with the as-prepared aligned nanotubes [53].

Droplet probe AFM

Modified AFM was introduced to precisely quantify the wetting properties of the superhydrophobic butterfly wing and underwater oil-repellent poly(sulfobetaine methacrylate) (pSBMA) superoleophobic surfaces [126]. Here, gold-coated tipless cantilevers were used, where circular pads were created. Water droplet and silicone oil droplet were generated to characterize superhydrophobic and superoleophobic surfaces, respectively as shown in Figure 2.6. This technique is called droplet probe AFM. Using this technique, it is also possible to spatially map chemical heterogeneities on the surface with micron lateral resolution.

Force tensiometer

This new technique is employed by DataPhysics to record adhesion force and to characterize the liquid-solid interaction using a high-sensitivity micro-electronic mechanical balance system or commercially termed as tensiometer. Here, the sample stage goes into the vertical motion to perform the formation and destruction of solid-liquid interface. Net vertical force experienced by the force sensor is continuously recorded with respect to the position of the substrate and time. The first measure-
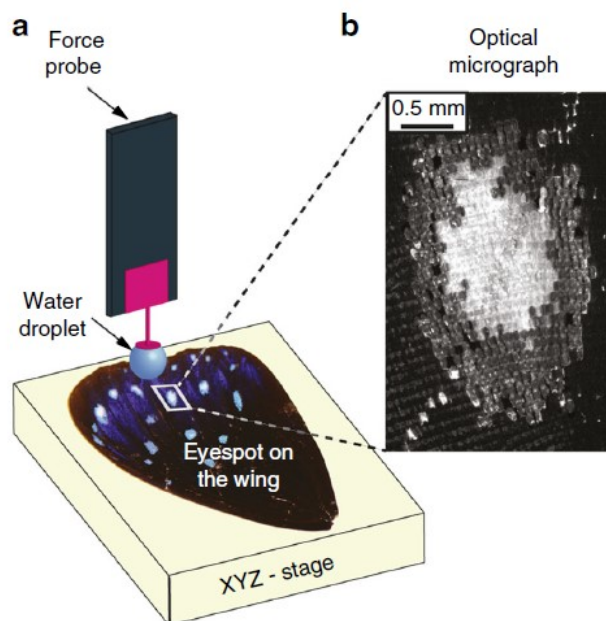
Figure 2.8: (a) Schematic diagram of the microscope, (b) Optical micrograph of scanned eyespot area on wing [127].

ment of the force-distance curve was performed in 2005 by Meihua Jin and coworkers [53] (personal correspondence and refer to Dr. Kashmiri Lal Mittal). They reported superhydrophobic polystyrene (PS), composed of greater than 6,000,000 aligned nanotubes per square millimeter. Figure 2.7 shows the force-distance curve recorded by performing a series of steps using a ring holder of a fixed droplet volume. Here substrate has been brought into the vicinity of the droplet for the solid-liquid attraction at the end of process 1. Later, the sample stage was gradually moving downwards and the force is increasing in process 2 and reached its maximum at the end of the process. Finally, the balance force decreased immediately when the drop is detached from the surface in process 3 and the drop is detached. The complete process was recorded using an optical microscope lens and a charge-coupled device (CCD).

Scanning droplet adhesion microscopy

This technique (Figure 2.8), pioneered by Villi Liimatainen et al. [127] is used for obtaining wetting map on non-flat and biological surfaces. 1 mm diameter SU-8 discs were used for holding the probe droplet, by shooting sub-nl droplets using the piezoelectric microdispenser. The wing of the striped blue crow butterfly was selected due to its numerous scientific interest [128, 129] and was placed on a multi-axis sample stage; brought in contact (snap-in) with the droplet and then retracts until it separates (pull-off force) in the vertical direction.

2.3.2 Lateral force measurements (Parallel to the TPCL)

The force that resists the lateral motion, experienced by a liquid droplet sitting on a solid surface is called droplet retention force [14]. A few studies [6] have demonstrated a direct measure of lateral adhesion forces to slide the liquid droplet. This is important for many applications like paint spraying [130], condensation and water collection [131] where the lateral motion of the droplet dictate the outcome of the process. In 2009, centrifugal adhesion balance (CAB) was developed [132], which can induce or independently manipulate the normal and lateral forces between a liquid drop and a surface, using the combination of centrifugal and gravitational force. Here, the droplet sitting on the solid surface is subjected to centrifugal rotation, perpendicular to gravity. As ω (the angular velocity) gradually increases until at some critical ω the drop moves. Eventually, lateral and normal forces can be calculated based on the critical angular velocity and weight of the droplet.

Next, we have droplet adhesion force instrument (DAFI) [50], consists of positioning a capillary in the centre of a liquid droplet, sitting on a surface, where drop is subjected to move sideways against the capillary at a constant velocity. The motion of the substrate is accompanied by a deformation of the drop or we can say deflection in the capillary, as it sticks to the drop. The droplet is set into translational motion

relative to the substrate, if the drop could overcome the lateral adhesion (F_{LA}). This deflection of the capillary is recorded with respect to position (D) and hence, lateral adhesion force acting on the drop can be calculated by $F_{LA} = \mathcal{K}\text{D}$, where $\mathcal{K}$ is the spring constant of the capillary.

2.4 Comparison of measurements methods

This section draws the comparison of above-mentioned techniques based on their end-user applications and limitations. There are a couple of methods that can be used in different surrounding mediums. For better understanding, we have classified them into two categories of surrounding fluid medium, one is air medium and the other is liquid medium.

2.4.1 Air medium

- **Atomic Force microscopy (AFM)**

  The family of scanning probe microscopy methods for surface imaging, and studying surface forces has developed over the 35 years. Atomic force microscopy force-distance curves have become a fundamental tool in several fields of research such as surface science, material engineering, biochemistry, and biology [133]. For example, in pharmaceutical companies, drug deliveries have become increasingly important. E.R. Beach and coworkers [134] measured the pull-off force between pharmaceutical powders and substrate materials used in dry powder inhaler devices. These techniques are incorporated into the family of microscopic methods [123].

  However, there are several problems associated with this technique, such as the lack of reliable methods to determine the tip shape and dimensions, which introduces the uncertainties in the attractive forces. The use of a big colloidal tip of known dimensions is not an effective solution to this problem, because

one of the major advantages of the AFM, namely the capability of probing local interactions on a very little area, is lost. As we also discussed the droplet probe AFM technique in the previous section, it is noted that this technique is only limited to submillimetric droplet size and to measure small ranged forces. It is well suited to characterize surfaces with low adhesion properties such as superhydrophobic surfaces but less functional with high surface energy surfaces.

- **Force tensiometer**

  Several studies have been done to utilize microbalance for performing adhesion force measurements on modified surfaces like hydrophobic or superhydrophobic, self-cleaning or anti-icing surfaces. For example, Yujin Sun *et al.* [68] quantitatively studied the solid-liquid interaction for textured surfaces with pores and pillars on PDMS. Later, adhesion forces on hydrophobic PDMS surfaces patterned with the concentric rings were also studied and discussed the visualization of contact line conformations. They examined the surface tension force and Laplace pressure force with varying droplet base diameter [84, 135]. Furthermore, in most of the studies, it is observed that force measured at spreading and drop detachment are related to advancing and receding contact angles respectively. Since the invention of this technique in 2005, researchers have been used to characterize surfaces, also to find the correlation between measured adhesion force and contact angle measurements, unfortunately, the procedure to use this technique for adhesion force measurements has not been studied in details yet. Furthermore, there is no discussion on the influence of parameters such as droplet volume, configuration of droplet holder, surrounding medium on measured adhesion force using tensiometer.

- **Centrifugal adhesion balance (CAB)**

  Two techniques have been discussed to measure adhesion force in the lateral

motion manner. One is the CAB technique, and the other is DAFI. CAB technique does not comment anything on the surface uniformity of the surface and uses external forces to produce lateral forces to slide the liquid droplet sitting on the solid surface.

- **Drop Adhesion Force Instrument (DAFI)**

  The major limitation of this method is that it only applies to drops with less than 2 μl volume. Furthermore, this method will be helpful provided that the adhesion between the drop and the capillary is larger than the lateral adhesion between the drop and the solid surface.

Water medium

It is also important to study the surface wettability and adhesion in liquid medium due to the wide range of underwater applications such as self-cleaning of marine equipment, oil/water separation and small oil droplet transportation [136–139]. Abundant studies have been achieved to fabricate and design structured dependent oil adhesive surfaces to control the oil adhesion in water. However, characterization of these surfaces is still limited to contact angle measurements. Contact angle measurements don't do enough justice to these surfaces because of various reasons. First, these surfaces have micro and nanoscaled textures on their surfaces, which implies different local contact angles. However, what we get from sessile drop goniometery is the apparent contact angle. Second, this characterization is optical-based technique that limits to analyze pinning or depinning effects at local regions due to its low resolution limit. Here we have discussed studies in the literature employing force tensiometer to study force-distance curve for liquid medium studies.

- **Force tensiometer**

Recently, researchers have paid attention to utilize direct measurement of adhesion

force technique using a force tensiometer to quantify the wettability of superoleopho-bic surfaces. For example, Enshuang Zhang *et al.* [83] fabricated underwater super-oleophobic Ni/NiO surfaces with controllable morphologies using electro-deposition process. Force-distance curve was recorded using microbalance to characterize these structure-dependent oil adhesion surfaces, and pull-off forces were measured. Similar characterization has been achieved to fabricate artificial high-energy coating to pro-vide underwater low adhesion surface properties [140]. These studies majorly focus on pull-off forces to validate the low adhesive properties. However, the process for directly measurement of these interactive forces in air and water medium has been the same in the literature. If we compare force-distance curve obtained for air medium and liquid medium for any different solid-liquid interface, we can totally agree that the initial force exist in case of air medium, is going to be spreading force only; when characterizing substrate comes in contact with liquid droplet. However, it's not the same observation in case of liquid medium. Even before the formation of solid-liquid interface, force sensor experiences some other forces, might be buoyancy force or hydrostatic pressur force, which never discussed in the literature so far.

2.5 Conclusion

In the beginning, we have focused on the measurement of interactive forces between two forces recorded in early 1900s. Later we discussed about the invention of AFM and its applications. This technique is modified and have been also used to character-ize surfaces with a liquid droplet. Furthermore, different measurement methods have been briefly discussed and compared to record solid-liquid interaction. Therefore, after doing extensive literature review of measurement techniques used in the past to record force-distance curves and to study solid-liquid interaction, this project focuses to study the adhesion force measurement using a force tensiometer. We have pro-posed a protocol to accurately and precisely measure adhesion forces between a liquid

droplet and a solid surface in any fluid medium. This work scrutinizes the operating parameters such as drop volume and magnitude of compression which can directly affect the adhesion force curve. We also discussed the components of adhesion force, which are surface tension force and Laplace pressure force separately with respect to change in these operating parameters.

Chapter 3

Adhesion force quantification for a solid-liquid interface

3.1 Abstract

Surface wetting and surface adhesion has gained major attention due to their numerous industrial-based applications such as droplet transportation, superhydrophobic and self-cleaning surfaces. Contact angle measurements are a well-known method to quantify the surface wettability and adhesion, however, the clarity of direct measurement of these interactive forces is still limited to theory. There are some findings that measured the adhesion force using a force tensiometer and studied the modified surface properties of the surface based on adhesion force, yet the details of the technique are still under research. Therefore, we present a protocol that provides the guidelines to directly measuring adhesion forces between a liquid and a solid interface using a force tensiometer. We have proposed precise and necessary steps to produce reproducible and repeatable results to quantify the magnitude of adhesion force directly. Moreover, this work takes into consideration the effect of the surrounding medium on adhesion force, and provides a procedure to obtain absolute and accurate adhesion force in liquid medium as well.

3.2   Introduction

The capability of a liquid droplet to adhere to a solid surface in a surrounding fluid medium has intrigued many researchers over the past few decades [20]. For example, in nature, hierarchical roughness at nano-scale on lotus leaf prevents water to interact with the underneath surface to keep it clean and unaffected [141], the ability of insects like beetles and blowflies to make an attachment with solid surfaces by releasing the fluids from pads [142] or secrete adhesive by plants' glands to digest small insects or fruit flies [143], inspired authors to fundamentally understand the wetting and adhesion properties of a drop sitting on a solid surface. These studies help material scientists, physicists, and chemists to prepare synthetic analogs such as superhydrophobic/self-cleaning surfaces [19, 144] for many industrial-based applications like dropwise condensation, self-dirt removal, offset [145] or inkjet [146] printing, spray coating, and anti-icing surfaces [147], to name a few.

For instance, in offset printing, understanding of wetting and de-wetting of ink on different printing surfaces is crucial, and several parameters can compromise the printing process, from the dynamic surface tension of ink to adhesion between the ink and impression cylinder and between the ink and the paper [148].

Therefore, it is essential to characterize the wetting properties of physically or chemically altered solid surfaces interacting with liquid droplets in a given surrounding fluid medium. The sessile-drop technique [149] or the dynamic contact angle measurements [38] is the most widely used techniques in the literature for surface-wetting characterization. In both the techniques, static and dynamic contact angles are measured based on Young's equation of surface/interfacial energies and increasing/reducing drop volume method respectively, using a goniometer. However, the existing literature derived from above-mentioned CA results lacks insight into a force interaction between a liquid droplet and a substrate, which could contribute effectively to the wetting science [20].

Meaningly, there are some important factors to take into consideration to provide the most in-depth description of interactive forces. To provide accurate and reliable results, it is paramount to establish a protocol, which includes steps necessary to be taken to prepare the sample and to establish variable experimental parameters. Here, we present the process to record the adhesion force curve between a liquid droplet and a solid surface in a fluid medium. It consists of five-seven significant distinctive steps. These steps are in the sequence of approaching, spreading, compression, retracting, and separation as depicted in Figure 3.1.
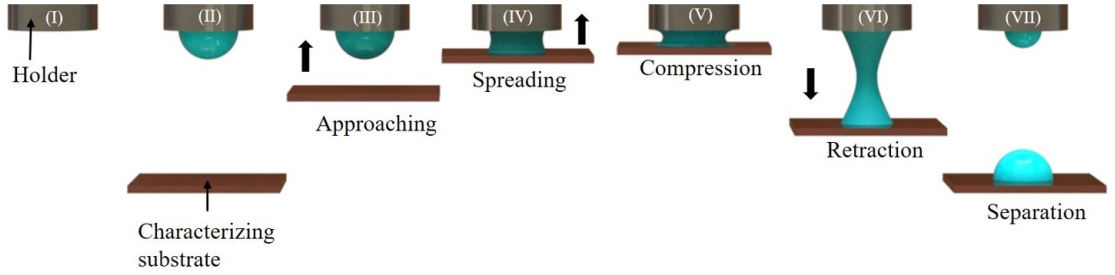
Figure 3.1: Schematic of different steps (I to VII) involved in adhesion force measurement between a characterizing solid-liquid interface in a given fluid medium, air, or liquid. The load cell/force sensor records the force experienced by the holder at all times. I: Sample holder is attached to the load cell; II: Drop of a fixed volume is generated at the tip of the holder facing towards the substrate; III: A substrate is going into a motion towards the liquid droplet until the solid-liquid interface forms. The distance between an interface of the holder and a substrate is named separation distance; IV: Equilibration of the solid-solid-liquid interface without changing the separation distance; V: Forceful spreading of a liquid droplet over the solid surface (compression) to attain uniform spreading; VI: Stretching of the liquid interface VII: Droplet breakup or detachment.

Adhesion force, experienced by the force sensor is the result of a combination of two forces, namely surface tension force acting along the perimeter of the TPCL and Laplace pressure force due to the pressure difference across the liquid-gas interface [150].

$$F = 2\pi r\gamma \, sin\theta - \pi r^2 \, \triangle \, P \tag{3.1}$$

where, F is the total vertical adhesion force, experienced by the force sensor, γ is

the surface tension or interfacial tension of probe liquid in the air or liquid medium, respectively, θ is the contact angle of probe liquid measured with the solid surface, r is the droplet base radius and $\triangle$ P is the Laplace pressure.

3.2.1   Adhesion force measurement using force tensiometer

The method of measuring adhesion force in this protocol, as shown in Figure 3.1 is performed using a force tensiometer. In 2011, Samuel *et al.* [41] recorded adhesion force between a liquid droplet and a solid surface using a micro-electronic mechanical balance or commercially known as force tensiometer, where a platinum, ring-shaped holder is attached to suspend the liquid drop. They concluded that the forces measured during the solid-liquid interactions during spreading and pull-off are directly correlated with advancing and receding dynamic contact angles, respectively, measured independently using a goniometer. Their research findings inspired other academics to study these interactive forces for modified solid surfaces using a force tensiometer to obtain desired surface functionalities [135]. It is also found that the most stable state of a liquid droplet sitting on a rough and anisotropic surface is when its shape would be axisymmetric [151].

However, the process of generation of a solid-liquid interface, such as the rate at which the interface is being formed and modified or the surface energy of the drop holder, is not mentioned or described at any level of detail. Additionally, there is limited understanding of the role of commonly required operating parameters like liquid volume, retracting speed, the magnitude of compression, and surrounding medium on adhesion force measurements [152]. These factors have an explicit and significant influence in quantifying the true magnitude of maximum adhesion force, as demonstrated in the next Chapter 4 of this thesis. Hence, in this protocol, comprehensive instructions to generate reproducible and repeatable (R & R) adhesion force measurements are provided.

3.2.2 Development of the protocol

Using this protocol, adhesion force between different solid-liquid interfaces in air and liquid mediums was recently measured in Chapter 4. This work showed that the operating parameters such as drop volume, compression value affect the magnitude of the surface tension force component, Laplace pressure force component, and eventually total adhesion force. It is observed that variations in these parameters vary the droplet base diameter and hence, affect total adhesion force. Thereafter, component forces and total adhesion force were normalized with their corresponding power of droplet base diameter to negate the effect of operating parameters. The influence of the surrounding medium by changing from air to water was analyzed by performing experiments with silicone oil can also be seen in the next Chapter. The procedure of measuring interactive forces in liquid media is also mentioned in this protocol in a later section.

3.2.3 Comparison with other methods to measure adhesion force

Various methods have been reported to measure the interactive force between a liquid droplet and solid surface directly, in the past few years [153]. To provide a clear understanding, these methods have been organized into two categories, namely the vertical and lateral force methods. Vertical force method is derived where a liquid droplet is subjected to a vertical motion to interact with a solid surface; hence, force measured during retraction is referred as adhesion force [14]. On the other hand, lateral force method is commonly explained when a liquid droplet sitting on a solid surface, slides over experienced by a lateral motion, the force that resists this motion, is termed as retention force [14]. There are various techniques introduced to slide the liquid drop over the solid surface. For example, lateral adhesion force is measured using the centrifugal adhesion balance technique, where the combination of centrifugal

and gravitational forces was used to slide the drop-down [50].

Furthermore, in the vertical force method, the two most widely used instruments, to characterize surface wettability in terms of adhesion force, are droplet probe atomic force microscopy (AFM) and microbalance or a force tensiometer. Dan Daniel *et al.* modified the AFM technique by replacing the canteliver tip with a micro-sized liquid droplet of 40-wt% glycerin-water, attached to the AFM cantilever [154] to measure adhesion and friction forces. They have measured the adhesion and friction force for superhydrophobic surfaces and underwater oil-repellent polyzwitterionic surfaces, and spatially resolve topographical and chemical heterogeneities with micron resolution [126]. In the case of a tensiometer, as we discussed above, the liquid drop is brought in contact with characterizing substrate and the total vertical force experienced by the load cell is recorded due to formation and detachment of the solid-liquid interface. Table 3.1 provides an overview of some of the measurement methods and discusses some measurement techniques used to characterize surface wettability.

Table 3.1: Different adhesion force measurement methods.

Method	Description	Advantages	Limitations
Vertical force methods			
Drope probe AFM	Water droplets and silicone oil were deposited at the gold-coated tipless cantilevers to measure surface forces.	Ability to spatially map chemical heterogeneities on the surface with micron lateral resolution.	Limited to measure only small ranged forces. Difficult to measure solid surfaces with high surface energies.
Adhesion Force using tensiometry	the characterizing solid surface brings in the vicinity of liquid drop and various steps such as spreading, compression, retraction are performed to quantify adhesion force value.	Ease of automation. Purposefully designed for inkjet printing application.	Subjected to unreproducible results if accurate and detailed protocol is not followed.
Lateral force methods			
Centrifugal adhesion balance (CAB)	It is the combination of gravitational and centrifugal forces to slide the drop down. Theses forces are capable to decouple the normal and lateral forces and manipulate them independently to drive the drop sitting on the surface.	Beneficial for applications such as drag reduction, condensation, and spray coating. Can measure lateral adhesion forces for both sessile and pendant drop.	It is time consuming as it requires to collect information from a large area which demands multiple measurements. No data about the surface uniformity of the surface . Uses external forces to produce lateral forces.
Drop Adhesion Force Instrument (DAFI)	Drop Adhesion force Instrument works on the principle of the deflection of the capillary that is stuck in a liquid drop sitting on a solid surface.	Highly sensitive instrument. Able to determine both static and dynamic lateral force.	Only useful when the adhesion between the drop and the capillary is larger than that between drop and the surface.

Each measurement technique has its unique strengths and limitations and the most suitable technique will completely depend on the end-user application. For instance, to characterize the wetting and adhesion properties of superhydrophobic surfaces, the droplet probe AFM technique can be used due to its lower order of magnitude (nN), however, it is only suited to measure interactions with minimal point of contact. On the other hand, adhesion force-based measurements using a force tensiometer would be appropriate for any solid surface ranging from conventional surfaces or altered surfaces, and also surfaces with high surface free energy. They are best suited for applications like offset printing, self-cleaning properties, and droplet microfluidics. Adhesion force measurements using force tensiometer have gained interest and are extensively used due to its adaptability and convenience. Therefore, this protocol focuses on the accurate guidelines and procedures to measure solid-liquid interaction using a force tensiometer. Other than experimental research, there are several theoretical approaches to resolve lateral and vertical adhesion force. The protocol does not go into details on these models, details can be founded in the literature [26, 42, 155, 156].

3.2.4 Experimental design

The measurements in this protocol are performed using the force tensiometer where a sample holder for a test liquid/droplet is connected to the load cell and brought in contact with a solid surface to characterize surface wettability. The adhesion force is measured by bringing the solid surface in contact with a droplet using a fully automated machine or motorized stage. The drop should be generated at the centre of the holder's surface to avoid lateral forces.

The equipment is provided with a built-in application with several different commands to measure net vertical mass values/data points, corresponding to time, position, temperature, and other parameters that may vary with different manufacturers

and companies. These data points are exported later to analyze using either data plotting and graphing software or by other means preferred by the end-user. The obtained graph is the adhesion force curve versus time and/or position to study the various events that occurred during solid-liquid interaction. The results from at least five measurements performed with predefined parametric values are averaged to obtain reliable, reproducible, and repetitive results.

In addition, an optical setup is arranged to record the images/videos simultaneously and continuously, during the formation and destruction of solid-liquid interface. Relevant frames are later analyzed to determine the respective parameters corresponding to adhesion force such as droplet base diameter and contact angle.

Measure the adhesion force value of a solid-liquid interface as an average of at least five measurements. Clean the sample and a probe every time for new measurement and vary the position on the solid surface each time to gain information about the homogeneity of the wetting properties. Report the average adhesion force value for a particular solid-liquid combination with defined other parameters, as well as the standard deviation of the measurements.

3.3   Materials

3.3.1   Reagents

- Sample

- Cleaning agents - DI water (Milli-Q A10, Millipore), Isopropyl alcohol (2-Propanol, fisher chemical), ethyl alcohol (95 % EA, fisherbrand)

- Test liquids - DI water, silicone oil (D10 Paragon Scientific)

3.3.2   Equipment

- **Force tensiometer (K100, KR$\ddot{U}$SS Scientific Instruments Inc., Germany)**

Force tensiometer setup

A traditional commercial force tensiometer consists of the highly sensitive electromechanical balance system, motorized stage, and a software control various functions to enable measurements of surface tension, interfacial tension, dynamic contact angles, sedimentation, penetration, and custom measurements of force versus distance. The software is designed to perform various measurements based on end-user's input values. Customized series of tasks can be created based on operator's requirements and conditions. It also consists of standard built-in functions for common measurements such as surface tension of a liquid, interfacial tension of liquid-liquid interface, dynamic contact angles, and including but not limited to critical micelle concentration (CMC).
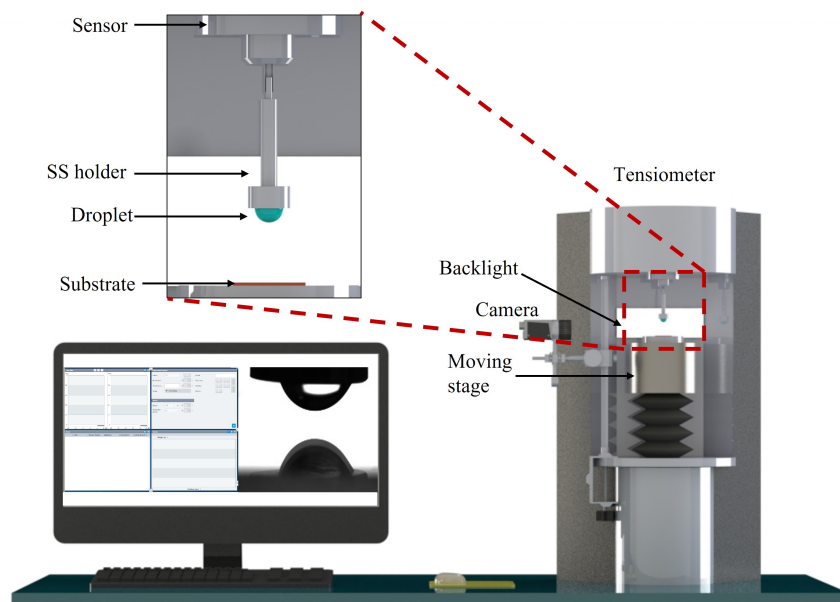
Figure 3.2: Experimental system used in this study. Force tensiometer consists of a load cell, a light source, an adjustable sample stage, a mounted camera device to record images/videos, and a data acquisition (DAQ) system to process the raw data and display the data simultaneously. The computer screen is set to display the results from the load cell and the imaging system simultaneously and continuously. Enlarged image shows the holder connected to force sensor and droplet is suspended at the holder facing towards the substrate.

Force tensiometer carries either an external control pad or build-in control buttons to regulate necessary operating steps before and after each measurement, if necessary, *e.g.*, stage movement, illumination, locking and unlocking of a force sensor, stirrer, ionizer, and others. It collects data based on two different measurements, one is the position-based measurement, where the force sensor collects data respective to the movement of the sample stage vertically. And the other is the time-based measurement, where data is recorded continuously with time, irrespective of stage movement/position. In this protocol, we used time-based measurement because, in position-based measurement, it only captures data when there is a change in the position of the sample stage, resulting in the loss of data points at equilibration of solid-liquid interaction. The location of the force tensiometer in the laboratory environment also plays an important role, and requirements are guided based on application and desired accuracy in the results, as it is a highly sensitive device. For applications where data needs to be collected at the lower end of the measurement range, *i.e.*, close to the resolution of the balance, it should be on a sturdy table or if possible, on a vibration-less table to prevent the disturbance of external vibrations. It is important because it can cause unwanted noise in the measurements and affect the standard deviation in the results. Not only vibrations from the supporting and surrounding structure(s) can cause disturbances in the measurement, even airflow from the room ventilation may introduce additional uncertainties, *e.g.*, sudden fluctuations in the raw data or continuous oscillations throughout the entire measurement, into the final result. It is recommended to keep the unit away from air vents. In addition, the surrounding air should be sufficiently clean of dust and vapor, which may adsorb on the solid surface or on the sample holder, or a liquid droplet, to avoid adverse effects on the measurements. The camera system is installed in a such way that sample holder is perpendicular

to the horizontal line of the field of view (FOV), as shown in Figure 3.2. The selection of the camera and its properties will be discussed in detail in the next section.

- **Camera system (KOS815, KR$\ddot{U}$SS Scientific Instruments (Shanghai) CO Ltd, China)**

Optical setup

The camera setup is installed to capture the interaction between a solid-liquid interface surrounded by a fluid. The end-user can have a selection of different camera options, and variables in capturing rate and resolution. The main purpose of installing the camera is to capture the dynamics of wetted length over substrate and the accuracy of the placement of the baseline, which, in the end, increases with resolution. Hence, it is advised to have high-resolution images and a droplet should occupy the entire field of view (FOV). The camera is installed in such a manner that the bottom of the FOV is parallel to the plane of a substrate. To capture variation in droplet base diameter, various adjustments can be done, such as tilting angle of the camera to clearly see the TPCL at the interface, distance between the substrate and the camera can also be adjusted in case of a fixed zoom, vary the focus configuration to achieve a clear view of the droplet sitting on the substrate and fulfill the requirements for the FOV. In addition, an external LED light source can be installed, opposite to the camera, to enhance image quality and contrast. However, the intensity of the light source should be optimized along with the lens focus to obtain the sharp drop-medium interface. Moreover, for liquid medium studies, the glass cuvette shouldn't be exposed to direct sunlight or other light sources with high intensity within the lab to avoid glare. Some general guidelines on camera settings are provided in Box 1.

Box 1 | Guidelines on camera settings

- **Frame rate**

  A camera system used to record the images/videos typically provides a fixed frame rate until a certain resolution past which the resolution reduces in favor of a higher frame rate. It is recommended to use the entire resolution of a camera; thus, keep the frame rate below the number when resolution reduces. Given the speed of motion for the samples stage, 50 frames per second (fps) provides a sufficient number of images for processing.

- **Magnification**

  The location of camera needs to be fixed at a recommended working distance from a camera system provider, given different configurations in terms of variability of zoom and focus. However, it is important to keep in mind that the obtained field of view (FOV) must fit the complete process from approaching to the detachment of the droplet. A pre-test may be necessary with conditions similar to the final test run.

- **Focus and tilting angle**

  Focus plays an important role to capture the accurate length of droplet base diameter. It is advisable to focus optimally on surface of characterizing substrate, by tilting a camera system, if required. Hence, when it interacts with the liquid droplet, the contact line along with liquid profile should stay in focus. The droplet should be aligned with the FOV to record both the contact points while spreading on characterizing substrate. The tilting angle can be set up to 4°.

- **Calibration**

  To measure the volume of the drop from the fitted curve, an image is calibrated with the diameter of the holder. It should be done each time the camera settings undergo changes in position, magnification, focus, or including but not limited to tilting.

3.3.3   Room conditions

All the measurements performed in this protocol are carried out at room temperature. The room conditions such as humidity and temperature are preferred to be steady. However, ±2-3°are not expected to affect adhesion force measurements. Surrouding

temperature can be monitored either with the build-in thermocouple within a force tensiometer or using external thermocouples connected to a DAQ.

3.3.4 Drop generation technique

As it can be seen in Figure 3.2, the holder is connected to a force sensor. Therefore, the working technique and configuration of the holder will directly affect the measurements recorded, experienced by the force sensor. We have studied three different holder configurations, where the drop is being generated within a sample holder or deposited directly/indirectly. All three configurations can be seen in Figure 3.3.

Regardless of configuration, it should ensure to provide minimum technical error and hindrance in the measurements to achieve reliable and reproducible (R & R) results. The key aspects to consider, while examining the holder, are to avoid any interference to the interaction of characterizing solid-liquid interface and not impart any design physical constraints to the droplet generation process.

SS holder:- A stainless-steel SS cylindrical/rod holder or SS holder is selected to suspend the drop facing towards the characterizing substrate. The diameter of the holder is maintained sufficiently large, in order to prevent any constraint to the spreading of liquid drop. To keep the liquid profile symmetric and to allow the droplet spreading freely, the holder should act as infinite plate parallel to the characterizing substrate. Therefore, we used holder with diameter of approximately 4.93 mm in both mediums to accommodate droplets as large as 9 μL.

Ring holder:- Inspired by the literature [41], a platinum/iridium ring holder is also used to perform adhesion force measurements.

Plate holder:- An inverted configuration is used like sessile drop approach, where droplet is sitting on the surface rather than suspended. This particular holder is inspired from the study of liquid bridge between two identical surfaces/plates [157]. Here, is the key difference between SS holder and plate holder; in plate holder the

drop is generated on the bottom surface and brings in contact with the upper surface to record adhesion force. This arrangement was adapted to investigate the role of spreading of liquid drop over the holder's surface and its effect on adhesion force, experienced by the force sensor.

Note:- Furthermore, the size of the droplet volume should be kept less than the capillary length scale, hence, it is recommended to use droplets with lower liquid volumes. On the other hand. the drop size should also be large enough to be analyzed via image processing software to avoid poor quality resolution images. Therefore, in our protocol, the drop volume is maintained between 2.5 µl to 9 µl. More details regarding the droplet volume can be found in the literature [38]. The exact details of the process to generate drop on these holders are mentioned in Box 2.

① — SS holder   ④ — Liquid droplet
② — Ring holder   ⑤ — Characterizing substrate
③ — Plate holder   ⑥ — Substrate
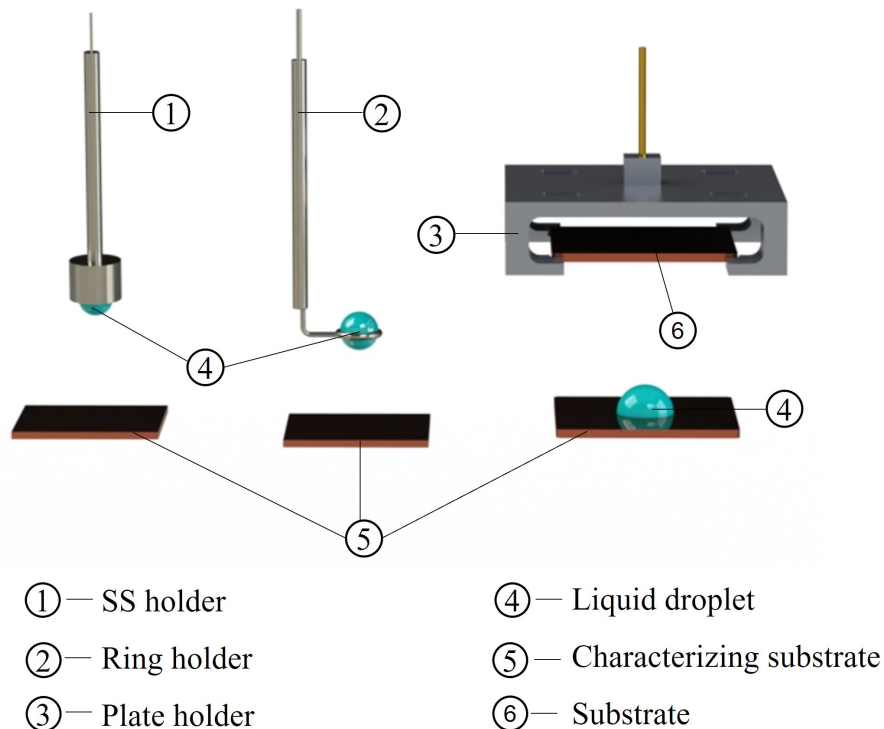
Figure 3.3: Three different types of holders used in this protocol: rod, ring, and plate. The material of rod and ring holders are stainless-steel and platinum/iridium respectively. For plate holder, same as of characterizing substrate has been used.

Box 2 | Drop generation process

- **SS holder**

  For SS holder, two different ways have tested to deposit the drop volume: one is for same (fixed) drop volume and the other one with varied drop volume.

  - ☐ **Fixed drop volume**

    1. A vessel filled with a test liquid, whose drop is to be generated (for example: water), is placed on the sample stage and is allowed to move vertically upwards to immerse the holder partially.
    2. A drop is formed at the tip of holder facing towards the sample stage, by immersing the holder in and out into the vessel at a constant speed.
    3. Fixed droplet volumes will be generated by maintaining same constant speed of immersion and cleanness of a holder.

  - ☐ **Varying drop volume**

    * Different values of drop volumes can be generated at the tip of holder manually with a syringe setup, where needle is positioned in proximity to the surface of a holder and syringe pump or analog is used to generate a drop.

  NOTE: The process to generate the constant droplet volume is fully automated here, which reduces the possibility of introducing human error to a minimum. In this method, force sensor is engaged to measure net mass of the liquid drop.

- **Ring holder**

  - ☐ Droplet of fixed or varied volume is placed onto a platinum/iridium ring using a syringe.

- **Plate holder**

  - ☐ A drop of fixed or varied volume is deposited by a syringe on the lower substrate.

  NOTE: The droplet volume can be confirmed by mass balance using the data either from a built-in force sensor in case of a rod and a ring or from an analytical balance for the plate holder to obtain reproducible results with constant volume. The secondary option is a curve fitting of a drop profile; however, end-user should keep in mind drop asymmetry.

After performing experiments using these three (3) different type holders, few things were observed for every holder. For the ring holder, as the drop is deposited manually, there is high probability to bring error in drop volume and the location it deposits. Also, it constraints the spreading of the droplet over fixed diameter of a ring and may cause asymmetrical liquid profile. In addition, due to the geometry of a ring itself where drop can freely move through the ring, liquid tends to bulge out while being in contact with the solid surface and may cause inconsistent measurements. And most importantly, it limits to use a fixed droplet volume and hence, would limit the study of varying drop volume effect on adhesion force.

For sessile drop technique, it introduces the human error while depositing the drop on the lower surface in terms of location to deposit, which could create imbalance to the system.

Hence, the SS holder is best-suited to produce R & R results, the drop generation is fully automated, and there is consistency in suspending a drop. Also. the liquid droplet spreads evenly on the surface and makes the liquid profile symmetrical and keeps a drop within the circumference of a rod profile. Hence, drop volume is software controlled and can be varied based on the requirements from the end-user.

Material surface preparation

It is advised that all the samples should be cleaned using a suitable solvent that does not damage or react with the surface. In this protocol, the samples are cleaned using distilled water passed through a water purification system (Milli-Q A10, Millipore), Isopropyl alcohol, and Ethanol. When performing measurements, the water in use must be used directly from the source and should not be stored in any container for a long time, as it may contaminate the water and eventually compromise the results. Further, after cleaning with 2-3 rounds of water and IPA or ethanol, care should be taken while wiping them off with tissues, as it may leave some tissue fibers/lints on it. Additional steps can be taken to guarantee the cleanness of a substrate using

compressed purified dry air or nitrogen from a tank or alternative source.

The samples should be either rigid or semi-solid, as changes of the topography of the sample while interacting with the droplet, when force sensor is engaged can affect the acquired adhesion force data. In case of lightweight samples such as Polyamide, there may be a need to attach to a glass side or directly to stage using a tape alternative means, *e.g.*, clamps, to avoid lifting off with the probe droplet.

Some important characteristic of the samples, used in this study, are listed in the Table 4.2. These values are measured right after the cleaning. Dynamic contact angle is measured using the Wilhelmy plate method with the water, as test medium.

Table 3.2: Surface properties of the substrate material used in this study. Standard deviation in the measurement of advancing (θ_{Adv}), receding (θ_{Rec}) angles, and surface free energy (SFE) is $\pm$ 1.53°, $\pm$ 1.32°and $\pm$ 2.04 mN/m respectively.

Substrate	Dynamic Contact Angle		SFE
	θ_{Adv} (°)	θ_{Rec} (°)	(mN/m)
Copper	86.42	63.86	34.58
PMMA	73.82	55.97	52.62
Teflon	118.37	80.67	11.70
Polyamide	83.43	47.32	44.84

Water is usually the preferred test liquid because of its high surface tension and resulted probability of surface wettability. In addition, it also has an important role in science and technology. Distilled water is preferable to guarantee absence of organic contamination, which will affect its surface tension and can introduce inaccuracy in the measurements. In this protocol, distilled water was also passed through a water purification system. It is important to assure that all the other equipment such as syringes, vessels, containers that come in contact with the test liquid or probe are clean. It can be verified by measuring the surface tension of water using a commercial

goniometer system with pendant drop technique for water or a Wilhelmy plate or Du Noüy ring technique using a force tensiometer. The resulted value is validated with the literature at experimental conditions. In this manner, we can ensure that the system is entirely clean before proceeding to the adhesion force measurement.

As we stated earlier to use water as probe liquid, we also used water as the surrounding phase for our liquid medium study. For that purpose, an optically transparent glass cuvette is best equipped for keeping water as a surrounding medium and guarantees drop access for an imaging system. For liquid medium studies, silicone oil is used as the probe liquid because it is non-polar and non-reactive.

3.4 Procedure

3.4.1 Measurement

In order to complete individual measurement, a series of commands needs to be programmed into a force tensiometer and it includes but is not limited to stabilization, zeroing, surface detection, setting speed of motion, control of a distance traveled by stage (compression value and current position), and data sampling rate. Those commands need to be entered in the correct order to successfully record the interaction between a liquid droplet and a solid surface. To the benefit of the reader, below is the detailed procedure of measuring adhesion force with time and distance in a fluid medium.

Study of different parameters

Table 3.3 provides summary of experimental parameters, *i.e.*, surrounding medium, compression value, compression speed, retraction speed, and surface detection speed. In order to control the drop diameter, compression distance is varied. Variable base diameter allows studying the net effect on maximum adhesion force by varying TPCL. Here, compression and retraction speeds have been kept at 1.0 mm/min, so that

process should only be dominated by surface forces [140].

Table 3.3: Summary of different parameters used.

Medium	Compression (mm)	Compression speed (mm/min)	Retraction speed (mm/min)	Surface detection speed (mm/min)
Air	0.0 0.2 0.3 0.4	1.0	1.0	5.0
Liquid	0.0 0.2 0.4 0.6	1.0	1.0	5.0

Air medium

1. Attach desired holder to the force sensor and tare.

2. ▲ CRITICAL STEP Generate a drop at the holder's tip using one of the methods previously discussed in Box 2.

3. After generating the droplet at the holder's tip, net mass is calculated for a droplet volume.

4. ■ TROUBLESHOOTING Tare the net force and move the sample stage closer to a liquid drop. Run the ionizer, if needed, for 5 - 10 seconds to neutralize any electrostatic charge present.

5. At this point, end-user can proceed with the measurement, defined as point O (see Figure 3.4).

6. ■ TROUBLESHOOTING Start data collection using time-based measurement

function at 50 Hz or similar function which enables data collection for force/-mass versus time.

7. Now the sample stage starts approaching the holder's tip in the upward direction to detect the droplet, depicted as movement from O to A.

8. At A, the force sensor detect the point of contact between a solid substrate and a liquid droplet, and instantaneously forces arise from A to B, experienced by the force sensor. A is called the onset of formation of solid-liquid interface and B is called the snap-in event. The force measured at point B is termed as snap-in/ spreading force.

9. Once the solid-liquid interface is formed, to attain the equilibrium and uniform spreading at TPCL, compression of a certain value (for example, 0.4 mm in this case) is provided, starting from point B to point C. For this, the sample stage starts moving further upwards to achieve a pre-set distance of compression.

10. At point C, compression ends, and retraction of the surface begins. Hence, the sample stage starts moving in the opposite (downward) direction. The force experienced by the load cell increases and achieves its maximum value at point D, termed as Maximum adhesion force or F_{max}.

11. After attaining maximum value, further withdrawal of the surface results in the decrease in adhesion force until point E, where drop detaches from the solid surface, from E to F. Finally, the droplet begins to snap off from the solid surface and the event is termed as pull-off event and force measured at E, termed as pull-off force. In the end, the measurement stops at point G.

    Note: The breaking up of the droplet into daughter droplets depends on numerous factors, such as solid-liquid interface, magnitude of compression and drop volume. The force at F is result of the transfer of the drop. For instance,

if the force at F is less than zero, it is clearly the indication of large residual

volume on the characterizing substrate. As in this case, force at F is almost

zero, as same as set initially, implies to merely transfer of droplet as shown in

inset F. Also the substrate is PMMA, which is transparent, explains the mirror

image of the droplet on the bottoms of all inset images in the Figure given

below.

12. ■ TROUBLESHOOTING the distance travelled value for retraction in the measurement should be kept as large with the purpose of complete drop detachment for all varied drop volumes.
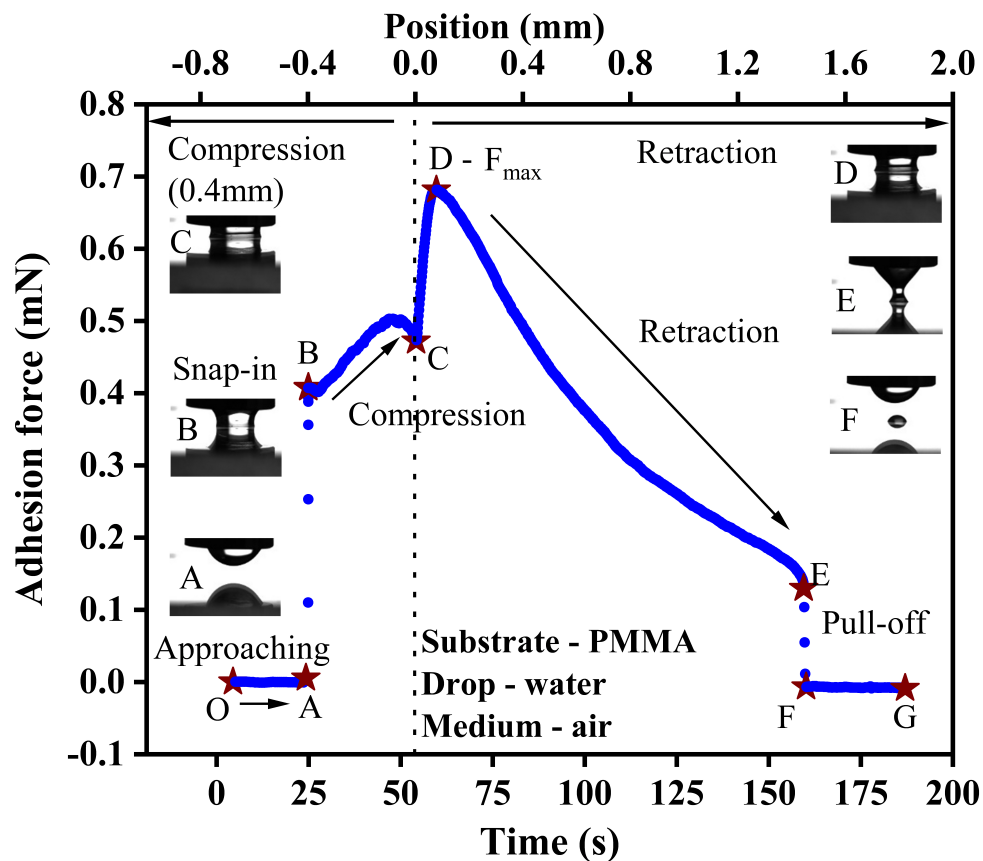
Figure 3.4: Typical adhesion force profile. Present profile is shown for the PMMA surface with water as medium for a droplet surrounded by air.

Liquid medium

In nature, there are exceptional natural biological surfaces, such as fish scales [158], nacre's shell [82] and lotus leaves' lower side [159], inspired many researchers to fabricate superoleophobic surfaces/materials for underwater applications, such as self-cleaning of marine equipment [160], oil/water separation [161], and anti-bioadhesive [162]. Therefore, it is essential to grasp the mechanism of wettability and adhesive properties of the surface in liquid / aqueous media as that of air media. However, there is limited context to provide a clear understanding for measurement of the interactive forces in liquid medium [83, 163] using the same technique. This work presents the essential steps to quantify absolute adhesion force value in liquid medium as well.

For the experimental setup for liquid medium studies, the in-house designed holder similar to the SS holder is employed to generate the oil drop inside the water medium. The holder is connected to the syringe pump (PHD22/2000, HARVARD APPARA-TUS) via a three (3) way valve and an oil drop can be generated of the desired volume at the tip of the holder as shown in Figure 3.5. There are some other factors that we should be considering while performing the liquid medium measurements, such as, buoyancy plays an important role during the movement of the holder or hydrostatic pressure from the water level in a cuvette, which affects the total net vertical force experienced by the force sensor.
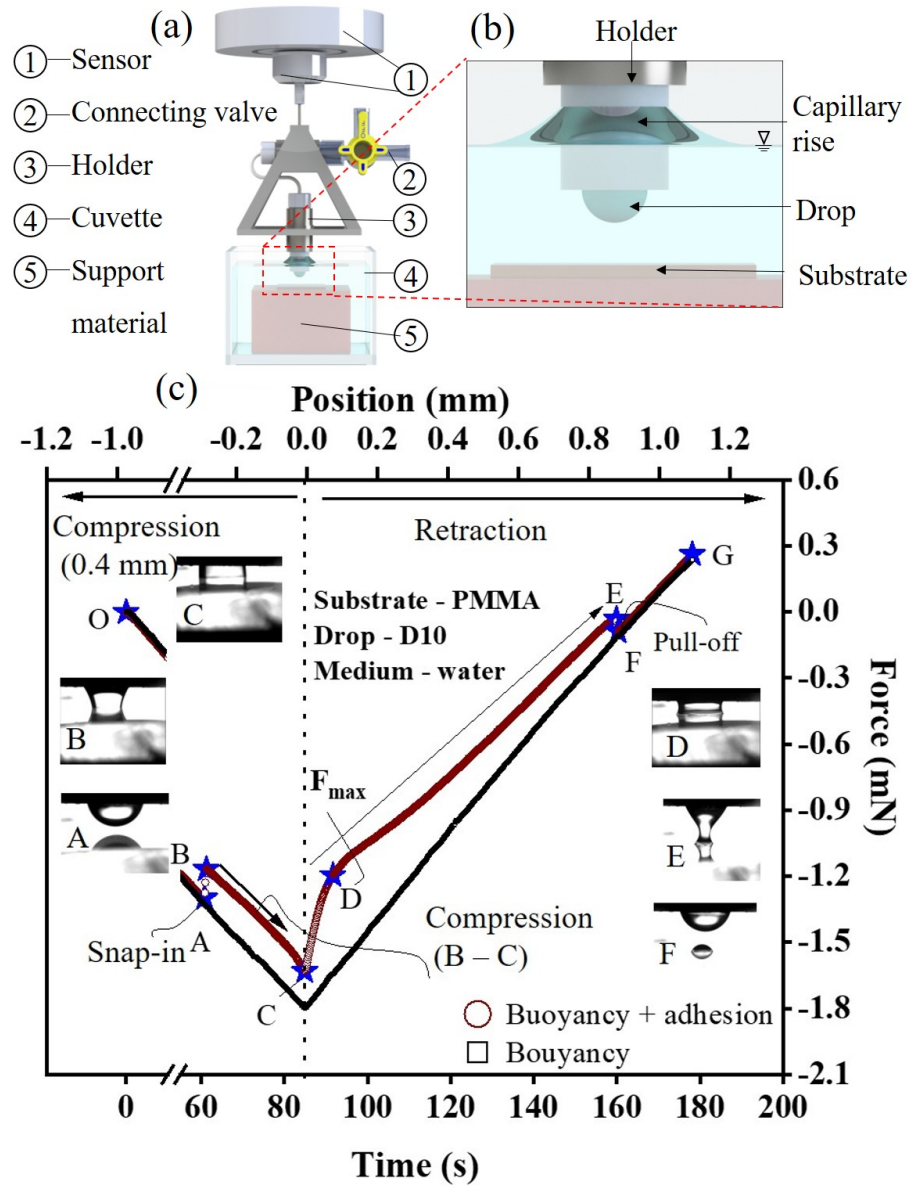
Figure 3.5: (a) Schematic representation of experimental setup used for water medium. (b) Enlarged image of the air-water interface is shown, where the capillary rise can be seen due to the movement of the holder inside/outside of the water medium. (c) Total force profile recorded in water medium for PMMA surface and silicone oil (D10). Here two experiments are performed: red curve (circled) is in the presence of substrate and the black curve (squared) without substrate with the same series of measurements.

Table 3.4 explains steps necessary to complete in order to obtain absolute adhesion force for a given solid-liquid interface liquid medium. It requires performing a single

experiment in two iterations. Iteration 1 is the formation of solid-liquid interface and Iteration 2 is without any solid-liquid interaction. To simplify that, for the same set of commands, the experiment needs to be performed twice, one with the substrate, and the other is without a substrate. After generating the oil drop inside the liquid media in both cases, at the same location (to keep the other factors exactly same), the sample stage starts approaching the oil droplet with or without substrate. in the first iteration, the solid surface starts approaching the oil droplet, solid-liquid interface forms, compression takes place and retracts till drop detaches from the solid surface, similar to the events performed in air medium. On there other hand, for iteration 2 the sample stage moves the exact same distance in both directions, similar to first iteration. After performing both the experiments and collecting raw data points, both curves are plotted in the same graph as shown in Figure 3.5 (c). The black curve (squared) represents when there is no formation of solid-liquid interface or in other words no presence of adhesion force. On the other hand, the red curve (circled) represents the events of interaction of solid-liquid interface along with other forces such as buoyancy and hydrostatic pressure.

Table 3.4: Procedure to record forces from the interaction of solid-liquid interface in liquid medium.

S. No.	with substrate	without substrate
1	Generation of an oil droplet in water medium at a fixed location for both cases. The location was kept the same in both iterations for consistency and ease of post processing steps.	
2	Solid surface starts approaching the oil droplet and travels to a distance "x" until the solid surface interacts with the oil droplet surrounded by the liquid.	Sample stage with water inside the cuvette starts moving upwards for "x" distance.
3	After the formation of the solid-liquid interface, the sample stage moves further up for a given compression distance.	The sample stage moves further up for the same compression distance in the absence of substrate. **NOTE:** It is important to keep clearance between the droplet and the bottom of the vessel to avoid any interactions with a drop.
4	After reaching point C (Refer to Figure 3.5 (c)), the sample stage starts retracting and till the drop separates from the solid surface.	Sample stage starts moving downwards the same distance.
5	The absolute adhesion force can be obtained by subtracting the force recorded without any formation of the solid-liquid interface (Iteration 2) from the measurements obtained with the formation of the solid-liquid interface (Iteration 1).	

3.4.2 Post measurement

- **Adhesion force curve:**

Once the total vertical force is measured for a solid-liquid interface, the data set points are exported in any suitable data format file, *e.g.*, Excel. Depends on a DAQ system, there might be a need to convert the mass (g) to the force (mN), obtained from the force sensor. It is required to initialize the force by zero, which can be achieved by taring up the net force before starting the experiment. The curve is plotted against elapsed time and position; hence,

double x-axis is chosen to plot the curve and keep the main x-axis to time. The curve starts from time equals to zero and corresponding position is set to 0 mm. It is also the same point, where the direction of the sample stage inverts, *e.g.*, after completion of compression step.

1. **Maximum adhesion force (F_{max})**

   F_{max} can easily be noted during performing the experiment. In this way, it is easily and directly to analyze the F_{max} for every repetitive experiments to achieve reliable and reproducible results. Also, F_{max} can be extracted from force-distance-curve.

2. **Normalized F_{max}**

   F_{max} is normalized with its corresponding droplet base diameter to study the effect of the three-phase contact line (TPCL) over adhesion force. This is achieved by measuring droplet base diameter (which will be discussed in the next section) and dividing it with measured F_{max}.

In a subject protocol, data analysis and graphing software (Origin, OriginLab 2021) is used to import and process data. For liquid medium studies, total force captured when there is no formation of solid-liquid interface should be subtracted from total force measured when solid-liquid interface formed and detached. It gives us absolute adhesion force between oil droplet and solid surface in liquid medium. Later steps are similar to air medium to be followed.

- **Contact angle measurement:**

A data acquisition process from the camera system needs to be synchronized with the data collection from force sensor, there should not be any time lapse between the video and force curve. In order to do so, exact time should be noted when video is started and stopped. Later, while analyzing the data, particular

force data point should be marked corresponding to the same noted time. In this way, duration of the experiment recorded by force sensor can be exactly synced with the duration of recorded video. Image where maximum adhesion force measured can be found using the time stamp from the force curve from tensiometer. Open the saved image and measure both contact angles (left and right) with the solid surface. Define the TPCL, *i.e.*, the line where a drop is in contact with the characterizing surface, either manually or using an automatic function within image processing software. The saved image was calibrated and post-processed with an image analysis software (ImagePro Premier 10.0, Media Cybernetics, Inc.) for the measurement of contact angle at F_{max}, advancing/receding CA. The contact angles can also be calculated using a customized program to detect the edge of the liquid profile at the interface and above the interface in the software itself. Also, any programming language can be used such as python or MATLAB to calculate the contact angle and droplet base diameter using built-in image processing packages.

- **Liquid transfer**

  Liquid transfer is explained as the residue volume left on the substrate after the drop detachment. This residue volume can be calculated based on the measurement of total drop volume at the beginning of the measurement. Force at F shows the mass of liquid drop left at the holder, which can be further calculated as droplet volume. Hence, by knowing the total drop volume, daughter drop volume of residue drop volume can be calculated.

3.5 Timing

- Record measurement and liquid medium using force tensiometer in

  - air medium: 5 minutes.

– liquid medium: 10 minutes.

- Analysis (required timing is software and desktop processing power dependent) to plot the curve in

  – air medium: 15 minutes.

  – liquid medium: 20 minutes.

3.6 Anticipated Results

This protocol simplifies the measurement of adhesion force for a wide variety of solid surfaces in any surrounding medium. The maximum adhesion force (F_{max}) provides insights into a given solid-liquid interface. Using this protocol, one can obtain adhesion force results in a repeatable and reproducible manner, as these results are solely dependent on the measurement of net vertical force experienced by a highly sensitive force sensor. Table 3.5 shows the measured F_{max} for different magnitude of compressions. Here, we can see that the standard deviation for adhesion force is in the range of experimental error which should be approximately 10 %. Droplet base diameter and CAs are measured using the image analysis software.

Table 3.5: Shows maximum adhesion force (F_{max}) for PMMA surface with water droplet in air medium with different magnitude of compression. Here θ in the table is the contact angle measured at F_{max}

Comp. (mm)	d (mm) ± 0.33	θ (°) ± 3.67	F_{max} (mN) ± 0.09
0.4	2.48	62.12	0.59
0.3	2.71	64.44	0.82
0.2	2.55	60.63	0.79
0.0	2.29	71.00	0.59

3.6.1 Comparison between different holders used
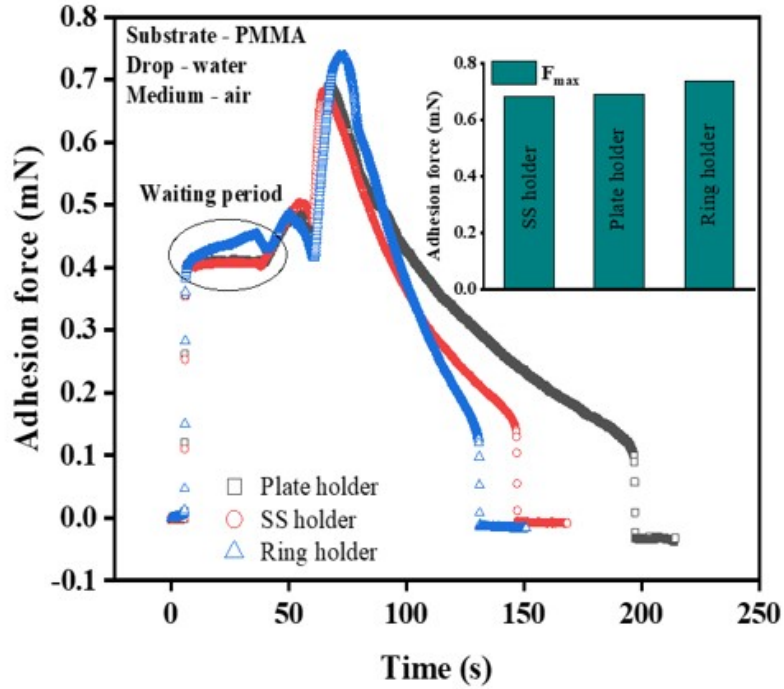
Figure 3.6: Comparison drawn between adhesion force curves obtained using three different holders.

Figure 3.6 depicts the different adhesion profiles obtained by using three different types of drop generation techniques between solid-liquid surface. The rod SS holder and plate holder showed similar results for maximum adhesion, spreading, and pull-off force events. On the other hand, ring holder curve shows larger value for F_{max}. These differences between the holder conclude that there is an influence of the interaction between holder's surface and droplet in the adhesion force curve. The magnitude of F_{max} of all these three curves can be seen from the inset curve, which has different values for different holders. Also, waiting period is shown in Figure for all three holders and there are some variations noticed in case of ring holder.

3.6.2 Adhesion force curve in liquid medium
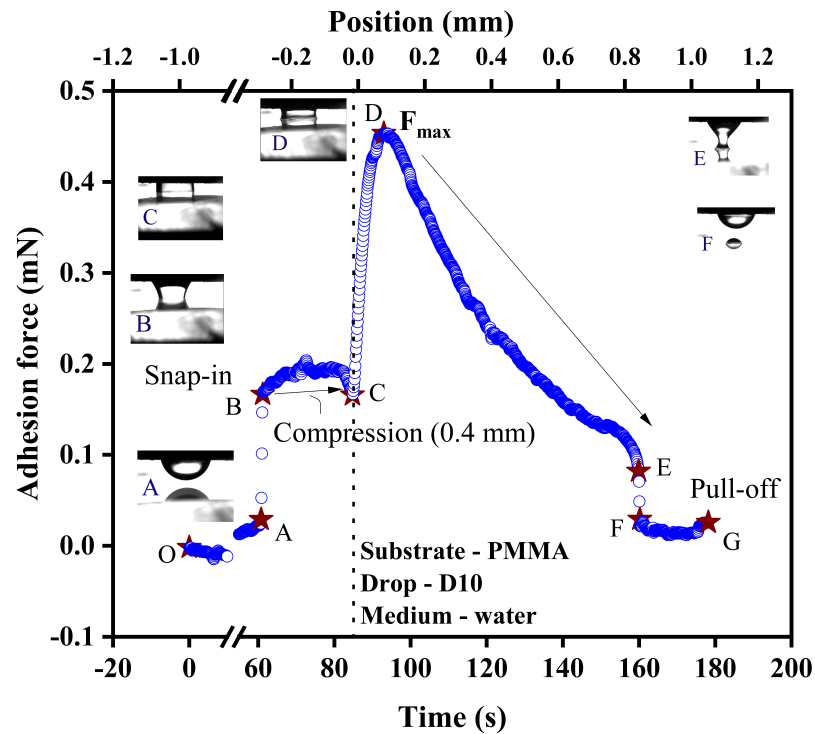
Figure 3.7: Adhesion force curve for PMMA surface with D10 oil droplet in water medium is plotted with respect to time and position. The absolute values of adhesion force has been calculated by subtracting other forces from total force, experienced by force sensor.

Here, absolute and accurate value of adhesion force is calculated by considering the other forces such as buoyancy force and hydrostatic pressure as shown in Figure 3.7. Underwater adhesion force profile is plotted using the same nomenclature used for air medium. The measurement starts at O in the same manner, where solid surface starts approaching the liquid droplet and comes in contact at A − B, spreads over the solid surface and snap-in/spreading force is measured. Oil droplet is further allowed to spread by providing the compression of 0.4 mm. From C, solid surface starts retracting and maximum adhesion force is achieved at D, followed by decrements in adhesion force and eventually, oil droplet get detached from E to F, termed as pull-off force. Table 3.6 is the troubleshooting table which provides tentative solutions to the possible issues and concerns during the adhesion force measurements.

Table 3.6: Troubleshooting table.

Step (medium)	Problem	Possible reason	Tentative solution
2 (Air)	Different drop volume using automated method with rod holder	Cleanness of the rod holder" or "Cleanness of a test liquid	Repeat cleaning steps or verify surface energy of a rod holder" and "Verify cleanness of a test liquid, e.g., perform SFT measurement.
4 (Air)	Attraction of droplet towards substrate without being in contact	Presence of electrostatic charges.	It is advised to run the ionizer before proceeding with the measurement. It is going to neutralize any charge present on solid surface, which might attract the water droplet because of its polar nature.
6 (Air)	Unwanted noise in the force curve.	Frequency at which data is collected is too high	The only solution to avoid unnecessary noise in the data is to optimise the frequency Hertz, depending on the instrument. If possible, place the instrument on an optical table.

12 (Air)	Incomplete drop detachment and consequently incomplete adhesion force measurement	Distance travelled in the downward direction is insufficient	To obtain complete force curve, it is recommended to set the distance as large (for example, 3.0 mm) which can accommodate all different drop volumes to completely detach the droplet and record force at F as well. This step can also be followed by the stop measurement process to disengage the force sensor.
1 (Water)	Overflow or no drop while generating	Pressure developed inside the tubing	For liquid media studies, it is advised to have 2-3 rounds of oil being overflown before proceeding with the final experiment after closing the valve. Now it would be much easier to open the valve and generate the single droplet inside the water. Once desired volume of oil droplet is generated, close the valve and disconnect the tubings.
2 (Water)	Different force curve for without substrate experiment	Different water level for every experiment	Keep the water level for underwater studies in cuvette exactly the same. It is important to have the same water level; otherwise, it will directly affect the Laplace pressure force.
	Substrate's baseline is not horizontal	Sample stage or camera are not leveled. Substrate is not flat.	It may be possible that sample stage is tilted by a couple degrees, due to which baseline shows tilted during video analysis. Verify substrate flatness and install shims if necessary. Level stage and/or camera unit.

Chapter 4

Study of adhesion force in different operating parameters and surrounding medium

4.1 Abstract

Studies on liquid droplet interactions with chemically, physically, or biologically modified solid surfaces like superhydrophobic, superoleophobic, or self-cleaning surfaces has become paramount due to growing demand from industrial-based applications. Thus, many literature resources focus on adhesion force measurement using a micro-electronic mechanical balance system. The adhesion force is a manifestation of the wettability of the substrate and interfacial tension of the liquid drop. However, adequate justification is not given to understanding the factors affecting the magnitude of adhesion force while measuring for a given solid-liquid interface. These operating parameters are drop volume, magnitude of compression and surrounding fluid medium. Hence, to demonstrate this, we have varied these operating parameters that resulted in corresponding different droplet base diameters and eventually influenced the maximum adhesion force in this study. The role of these factors on adhesion force was also analyzed from a theoretical standpoint, where the surface tension and Laplace pressure forces have been analyzed individually.

4.2   Introduction

Surface wetting and solid-liquid interactions are omnipresent in nature. These phenomena have been studied in science and engineering [19] due to their potential in many applications, such as droplet microfluidics [164, 165], self-cleaning [144], anti-icing surfaces [166], and electrophotographic printing [63]. One of the most emerging research areas in the wetting community is the surfaces that typically show high repellency towards a given liquid. This tendency to exhibit the liquid phobia is characterized by measuring the wettability ideally representing the higher contact angles ($>150°$) [167]. Keeping the wide ranges of applications for these surfaces such as drag reduction [168], anti-reflection [57], dropwise condensation [55], and self-cleaning surfaces [4], etc [14, 38]. Characterization of these surfaces such as merely goniometric, image-based wettability measurement are insufficient to relate the improved performance and surface wettability. Therefore, surface energy and adhesion force characterizations have become additional tools to quantify the performance indicator. The surface energy quantification is elaborately discussed in the literature[169–172] but similar detailed studies, focusing on the intricacies of the adhesion force measurements are missing.

Recently adhesion force measurement using a micro-electronic mechanical balance system [173] has emerged as a widely used technique to quantify the force between solid-liquid interface. It is worthwhile to mention that adhesion force measurement performed by Atomic Force Microscopy [174] and or Surface Force Apparatus [107, 175] developed by Israelachvili's group has gained increasing attention due to their varied and several industrial-based applications [176–178]. The magnitude of adhesion force with such tools is in the order of nN and is always assumed to be molecular level forces. The proposed study is at a larger scale (mN) and between liquid and solid interface.

Most of the commercially available adhesion force measurement tools are based

on electro-mechanical sensor or load cell technology. With this technique, the force-distance curve is analyzed while a new interface is being formed. In the case of solid-liquid interface characterizations, a drop is attached to the holder connected to the load cell/force sensor and the solid substrate is moved towards the drop to form the desired interface [41, 53]. Due to the sensitivity associated with load cell, the drop attached to the force sensor is always at a fixed position and a substrate is moved closer to the drop at a certain rate. The characterizing substrate is placed on the moving sample stage and during the vertical travel, a specific set of steps are performed. These steps are: engagement of a substrate with a drop, compression to ensure this engagement and formation of an equilibriated solid-liquid interface, retraction to quantify the adhesion force, and detachment to assure the complete disengagement of the load sensor from the solid. Starting from engagement to detachment, the load cell records one force component, mostly the normal to the solid-liquid interface. Thus, the force-distance or force-time curve is obtained similar to other measurements at different scales using AFM [179] and SFA [108].

Meihua Jin et al. [53] extensively used this method to characterize several newly engineered substrates and their adhesive properties in air and liquid media. The first time, they used this technique to study surface wettability on the superhydrophobic polystyrene (PS) layer, inspired by gecko feet. Also, Methylation functionality on glass surfaces that creates heterogeneous surfaces has also been characterized by performing the adhesion force measurements [152]. More recently Yujin Sun and coworkers [152] discovered that spreading force varies as wettability is changed and proposed a direct relationship between the hydrophobicity and adhesion forces. Apart from air medium studies, force-distance curves have also been measured for liquid medium measurements as well [83, 180, 181]. For example, Tianqi Guo et al. [163] demonstrated switchable oil-adhesion/high adhesive properties of honeycomb-like PAA structures both in acidic and in bases aqueous phases [181] and it can be

used for applications like controlling the liquid collection and transportation underwater. However, the force-distance curve recorded underwater in the literature showed the presence of some other forces even before the interaction of a droplet with a solid surface occurred. The presence of buoyancy force in liquid media might contribute to the total net force experienced by the force sensor. However, this aspect of the contribution of other forces has not been explored and quantified.

This work presents a critical analysis of commonly adopted procedures to quantify the adhesion force between a solid-liquid interface in air and liquid media. Furthermore, the role of these operating parameters like liquid volume, the rate at which the interface is formed and deformed, compression magnitude, and the surrounding medium, have a significant influence on the measurement. After varying these operating variables we raveled that, the force-distance curve is different for the same solid-liquid combination. We scrutinize the influence of these operating parameters and identified the appropriate ways to quantify the adhesion force by negating the influence of artifact.

4.3 Experimental Section

Experiments are carried out using a force tensiometer (K100, KR$\ddot{U}$SS Scientific Instruments Inc.) equipped with a microbalance with the resolution of 10 µg and an optical system (KOS815, KR$\ddot{U}$SS Scientific Instruments,(Shanghai) CO Ltd, China) to record adhesion force between a liquid droplet and a solid surface in the surrounding fluid medium. Figure 4.1 (a) shows the image of the experimental setup used, both in air and liquid medium. The optical system consists of a high-speed CCD camera and high-intensity backlight to record the images/videos simultaneously and continuously during the spreading and retraction of the liquid droplet over a solid surface. The camera is installed in such a manner that the sensor's side is aligned with a substrate. For camera settings, the frame rate of 50 frames per second (fps)

with a resolution of 640 x 480 pixels provides a sufficient number of frames (at least 30 fps) to process. Force tensiometer's sample stage driven by the brushless DC servo motor with a resolution of 16 nm and it was used to control the approach of the substrate towards the drop.

As shown in Figure 4.1 (a), a cylindrical/rod-shaped Stainless Steel (SS) holder, connected to the force sensor, is used to suspend the liquid drop in both air and liquid medium. In an air medium, a drop is generated at the tip of the holder by immersing it in and out of the vessel containing a test liquid placed on the sample stage. The entire procedure is automated to generate equal drop volume in every case. The confirmation of equal volume is achieved by image analysis as well as the net mass recordings by the force sensor. On the other hand, to dispense an oil droplet in a liquid medium, the in-house designed holder is used to assure that holder is simultaneously connected to the force sensor and tubing to the syringe/syringe pump (PHD22/2000, HARVARD APPARATUS). Oil is moved through the tubings and an oil droplet gets generated at the holder's tip inside the liquid medium, as shown in

Figure 4.1 (a) on the right hand side top corner. Tubing is detached from the holder after the drop generation process is complete. The force sensor records the adhesion force variation with respect to the position of the substrate in the z-axis. An exemplary liquid profile of a droplet in a fluid is shown in Figure 4.1 (b), where R, D, θ and r are the radius of curvature, neck diameter, the instantaneous contact angle (CA) of the substrate with droplet, and droplet base radius, respectively.

4.3.1 Materials

Adhesion force measurement is performed for different solid-liquid combinations in air and liquid media. Poly(methyl methacrylate) (PMMA), Teflon, Polyamide, and Copper (Cu) are the substrates that we selected based on their applicability it comes to the applications pertinent to adhesive properties. To avoid any ambiguity of soft
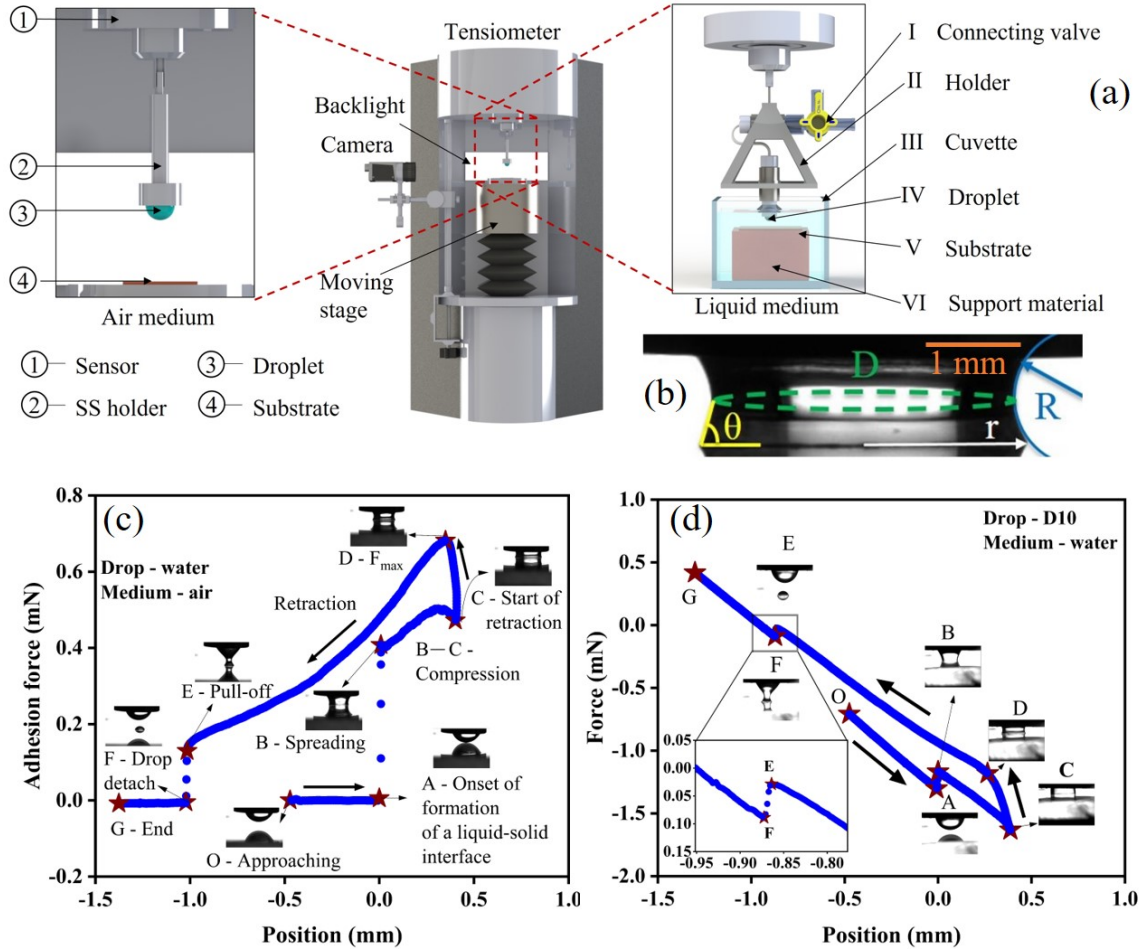
Figure 4.1: Explains the procedure involved to measure adhesion force between a solid-liquid interface using a force tensiometer, where: (a) shows schematic illustration of the adhesion force measurements method in air and liquid medium; (b) shows liquid profile at the maximum adhesion force point captured, where the contact angle, θ, droplet base radius, r, and principal radius R, and neck diameter, D are calculated; (c) shows adhesion force recorded with the position of the substrate for the water droplet and PMMA in air medium; (d) shows total force profile recorded in liquid medium for oil drop and PMMA substrate.

material characteristics we did not consider the Polydimethylsiloxane (PDMS), in this study. In this work, the substrates are cleaned using isopropyl alcohol (2-Propanol, fisher chemical) and ethyl alcohol (95 % EA, fisherbrand), followed by deionized water (MIlli-Q A10, Millipore). Finally, substrates are dried using lint-free wipes (Kimtech, Kimberly Clark) and compressed dry air. Oil-free air is also used to dry out the substrates and remove residual particles from the wipes. For the test liquids, water

(density of 1 g/cm^3) is used to form a drop in the air medium, and for liquid medium silicone oil (D10, Paragon Scientific) with the density 0.8286 g/cm^3 , lighter than water, is used as a probe liquid where water is present as the surrounding medium. Table 4.1 summarises the surface properties of substrates used in experiments.

Table 4.1: Surface properties of the substrate material used in this study. Standard deviation in the measurement of advancing (θ_{Adv}), receding (θ_{Rec}) angles, and surface free energy (SFE) is ± 1.53°, ± 1.32°and ± 2.04 mN/m respectively.

Substrate	Dynamic Contact Angle		SFE
	θ_{Adv} (°)	θ_{Rec} (°)	(mN/m)
Copper	86.42	63.86	34.58
PMMA	73.82	55.97	52.62
Teflon	118.37	80.67	11.70
Polyamide	83.43	47.32	44.84

4.3.2 Adhesion force measurement

Figure 4.1 (c and d) demonstrates the adhesion force-distance curve in air and water medium, respectively. The curve is obtained after performing all the necessary steps and each step is indicated by the symbol star in both the figures. These steps are, drop approach (O − A), formation of the solid-liquid interface (A), spreading (A − B), compression (B − C), retraction (C − E), detachment (E − F), and parking of the force sensor (F − G). The speed for all the steps mentioned here is constant at 1mm/min [157].

After the generation of a drop with the desired volume, the force balance is calibrated to zero (O). From O to A, the substrate approaches the liquid droplet, which resulted in no change in force. The instant, substrate comes in contact with the drop-air interface at A, the attractive forces surge between the liquid and the solid

surface. At this moment, the solid-liquid interface formation begins with a sudden increase in the force experienced by the load cell until B. This transition is called the spreading or wetting event [182]. The force-induced at B is termed as snap-in force or spreading force.

Once the solid-liquid interface is formed, to assure the uniform spreading and attainment of equilibrium at the TPCL, the forced wetting is performed. For this, the stage starts moving further upwards to allow the compression of a pre-set distance, *e.g.*, 0.4 mm, depicted as B − C on Figure 4.1 (c and d). During this stage, it is observed that the slope of the compression curve (B − C) changes along with the magnitude of adhesion force. At first, as the sample stage is moving upwards, it causes the forceful spreading of the droplet base diameter, which results in more attraction between the liquid drop and the substrate, and hence force increases further. However, once the surface energy of the system is minimized, further compression causes repulsion at the solid-liquid interface, leading to a decrease in adhesion force. This change in force from attractive to repulsive is an indication of complete spreading. This entire event (B− C) is also known as an advancing event [68], where a droplet advances over the surface. Adhesion force measurement necessarily starts from C where the retraction starts and it continues until the drop detaches from the solid substrate, process C − F. In this process, due to the pull away from the newly formed solid-liquid interface, adhesion force increases due to the change in state from advancing CA to receding CA [140], until it reaches the maximum at D (experienced by the load cell); hence, named as maximum adhesion force (F_{max}). Further withdrawal of the substrate, the force decreases due to the reduction in a droplet base diameter or TPCL and this stage is termed as receding event [173]. Finally, the droplet begins to snap off from the solid surface and the force of separation at this point (E) is referred to as pull-off force [41]. The complete detachment process is from E − F where complete destruction of the newly formed solid-liquid interface is attempted.

The force measurement ends at point G where the force sensors and holder motion stops. All the measurements in this study are carried out at a room temperature of 22°C.

Evidently, the transfer of a drop from the holder to the substrate depends on numerous factors such as surface wettability, droplet volume, compression, and surface properties of holder [40, 157]. For the studied solid-liquid combinations drop break-up with a residual drop on the substrate and daughter drop or satellite droplets formation after the bridge break-up is noticed. If the magnitude of force recorded by balance at point F remains the same as at O or A (at the beginning of the measurements after the drop generation), it is an indication of complete non-transfer of drop. It is to be noted that the residue volume and satellite droplets are very small, hence the force recorded after the detachment approximately to be zero (as initially set) in Figure 4.1 (c). The amount of droplet volume left on the substrate can be determined by the difference between the points F and A. If the force at point F is less than zero, it is due to the larger residual volume on the substrate.

For the liquid medium case (Figure 4.1 (d)), we have proposed a process with two iterations and in both the iterations all the steps are the same except for the formation of the solid-liquid interface in the presence of the liquid medium. In the first iteration, the force-distance curve is obtained similar to the air medium scenario, however, in the second iteration to quantify the buoyancy, the drop travels the same distance as the first iteration without forming the drop-solid interface. Pre-set commands for both the iterations are precisely the same and similar to the air medium scenario (Figure 4.1 (c)). These steps are as follows (Figure 1(d)) drop generation inside the liquid medium (O) at a predetermined distance from the substrate; drop approach (O − A), formation of the solid-liquid interface (A), spreading (A − B), compression (B − C), retraction (C − E), detachment (E − F), and parking of the force sensor (F − G). It is very important to note that, for the liquid medium force measurements,

70

even before and after the solid-liquid interface was formed or destructed, the force balance always experienced the force which is during the approach (O − A) and parking of the force sensor (F − G). In the case of the air medium, (Figure 4.1 (c)) for these two steps (before formation of the solid-liquid interface and after the complete attachment of drop), the force balance shows the constant force magnitude. This difference in air and liquid medium motivated us to add the second iteration to the measurement for the liquid medium measurements. Therefore, in the second iteration, where the solid-liquid interface formation and destruction are avoided, the sample stage is purposefully set to travel the same distance in both directions. Two forces buoyancy and hydrostatic pressure, which are absent in the air medium, are measured here. These two forces are dependent on the position of the drop inside the liquid medium. As the relative motion between the drop and medium starts, these two forces relatively change the force experienced by the force balance. Hence, non-zero increasing or decreasing force is recorded before and after the formation and destruction of the solid-liquid interface. Therefore, to obtain absolute adhesion force for a liquid medium study, another (without formation of solid-liquid interface) iterative process is necessary to subtract from the measurements obtained through the first iterations. For the repeatability and error analysis, for each solid-liquid-medium case, the data was collected at least five times with the same process and operating conditions.

4.3.3   Data plotting and image/video analysis

After recording the force-distance curve for a given solid-liquid interface in the air or liquid surrounding medium, data set are imported to the data analysis and graphing software (Origin, OriginLab 2021). On the other hand, image calibration is achieved before the repetition of every experiment using the holder's diameter. Also, it is noted that the images/videos are in the synchronization with the adhesion force

measurements. Videos are post-processed with an image analysis software (ImagePro Premier 10.0, Media Cybernetics, Inc.) to measure contact angle (θ) and drop base radius (r) or diameter (d).

4.4 Results and discussion

4.4.1 Role of commonly operating parameters and surrounding medium

The effect of operating parameters such as drop volume, compression magnitude, and surrounding liquid medium on the adhesion force curve is investigated. In this study, different adhesion force profiles are recorded to study the variation in droplet volume, compression magnitude, and medium role independently. Figure 4.2 (a) represents the three different adhesion force curves for PMMA and water in the air medium with different parametric conditions. The first curve, *i.e,* no compression curve (▲), is performed with 3 μl drop volume, where the substrate is immediately retracted away from the holder, after the spreading event at B, without executing any compression. Force starts to increase during retraction till it reaches F_{max} at D and eventually decreases until point E, where the drop gets detached from E $-$ F. It is worthwhile to reiterate, the forceful spreading is a common practice for all commercially available force tensiometers.

To study the effect of compression, results are obtained with the same operating parameters as performed earlier except for the 0.4 mm compression as depicted as compression curve (●) in Figure 4.2 (a). The results with and without compression is labeled as 'compression' and 'no compression', respectively in the same Figure. Same steps were performed until spreading event at B for both cases. Whereas, for compression case, compression of 0.4 mm starts from B to C that forcibly resulted in a larger base diameter. Afterward, the sample stage started retracting back from C $-$ E and obtained F_{max} at D. It can be observed that with compression the resulting F_{max}
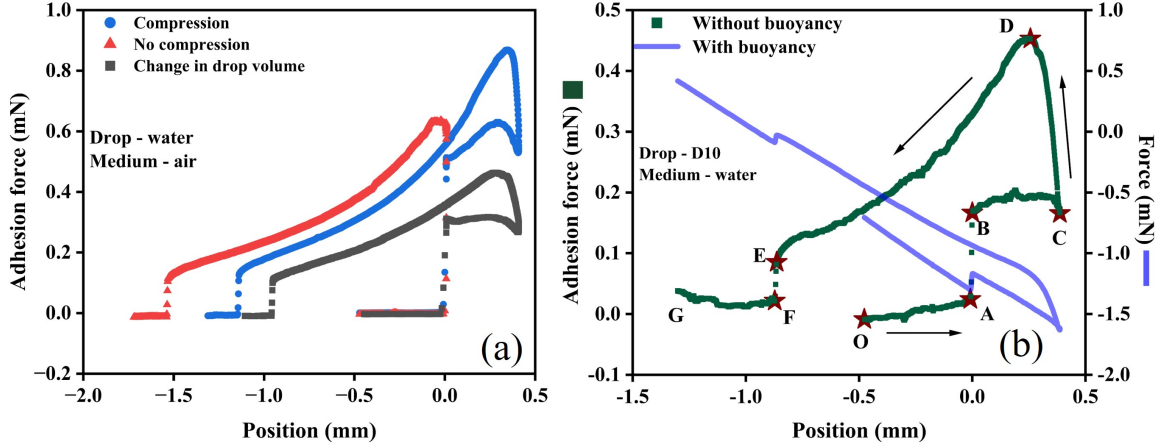
Figure 4.2: (a) Different adhesion force-distance curves are plotted for PMMA solid surface with water in an air medium under the effect of commonly operating parameters such as drop volume and compression. (b) absolute adhesion force and total force-distance curves are plotted for PMMA surface with oil droplet underwater to observe the role of buoyancy on adhesion force.

is larger. Here, it is evident that compression certainly has an impact of measured F_{max}, which is quantified as adhesion force in most of the similar studies in the literature [14, 41, 173].

To expand further, we also changed the volume to demonstrate its role in the force measurement result. For 2.5 μl drop volume curve (■), named as 'Change in drop volume' in Figure 2(a), the outcome is similar to the compression curve with a change in the magnitude of the instantaneous forces.

Apart from drop volume and compression, the medium also play a role while measuring the adhesion force. Using a two-step procedure from Section 2.2 for liquid medium measurements, Figure 4.2 (b) is obtained. Two different curves, with and without buoyancy, are obtained to negate the role of buoyancy and static pressure. After ignoring these forces, the force-distance curve profile is similar to air medium measurements. Hence, after the consideration of only interactive forces, Figure 4.2 (b) (■) shows the absolute adhesion force profile for PMMA surface and D10 oil droplet in water medium. From these three cases, namely, compression, drop volume and

surrounding medium, it is evident that adhesion force is sensitive to the operating parameters and detail investigation is required to comment on the correct magnitude of the adhesion force.

4.4.2 Role of operating parameters

A series of additional tests has been performed to study the relationship between the parameters and maximum adhesion force (F_{max}) in air and water medium.

Drop volume and adhesion force measurements

Figure 4.3 demonstrates different adhesion force profiles obtained by varying the drop volume from 2.5 µl to 9 µl for PMMA, Teflon, and PA surfaces with water droplets in air medium. In the case of water medium, the drop volume ranges from 3.5 µl to 10.5 µl for PMMA, Teflon, and Cu with oil droplets. While performing these measurements for a given surrounding medium, other factors such as the solid-liquid interface, the retracting speed, and magnitude of compression were kept the same. The magnitude of compression is set to 0.4 mm except for Teflon in the water medium, where the compression value is 0.6 mm. Here, a higher value of compression is selected because Teflon has a greater affinity with D10 oil droplet underwater and to observe the repulsive force, or to analyze the variation in compression curve (B − C).

By performing this study, some important findings came to highlight. To start with, the spreading force (B) increases by forming the interface of a larger surface area with an increase in droplet volume. Hence, the spreading base diameter is a function of drop volume, which eventually dictate the force experienced by the force sensor at B. As mentioned earlier, during the compression stage, *i.e.*, B − C, initially, attractive forces increase and then become repulsive at the end of the compression. However, as drop volume increases, due to larger solid-liquid interface repulsive forces are comparatively less, as shown in Figure 4.3. Followed by, once compression of the desired magnitude is achieved, adhesion force starts to increase during retraction,
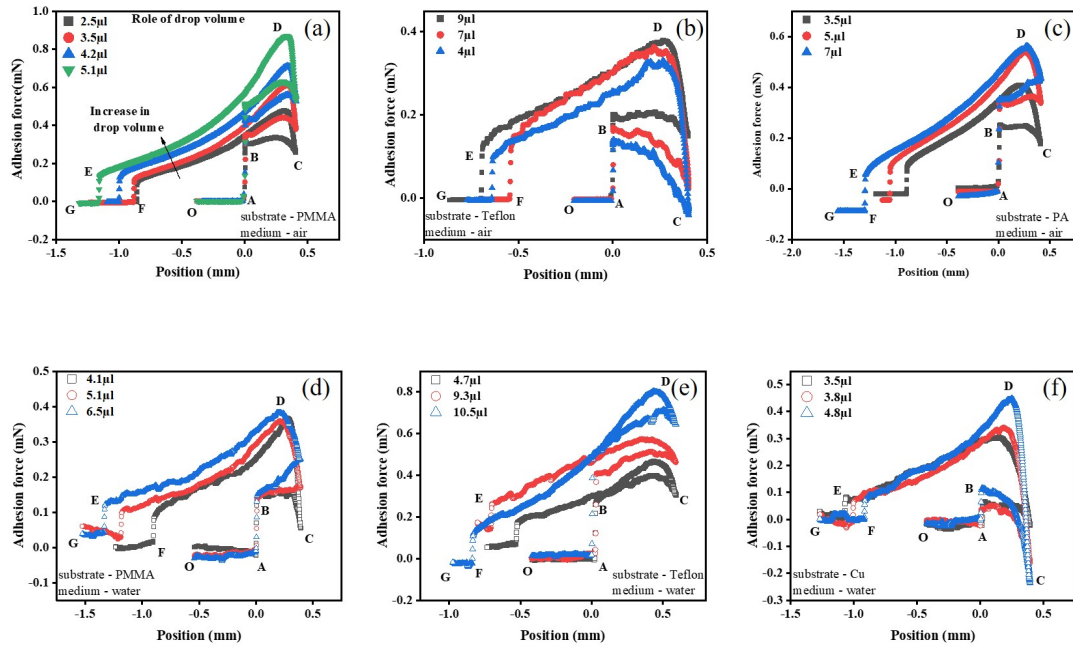
Figure 4.3: Force-distance curve recorded for varying droplet volumes between water droplet and (a) PMMA, (b) Teflon, (c) PA in air medium; whereas, between oil droplet (D10) and (d) PMMA, (e) Teflon, (f) Cu in water medium. Here the magnitude of compression is 0.4 mm except for Teflon in water medium with 0.6 mm of compression value.

and it can be seen that F_{max} increases with an increase in drop volume. This is also reflected in the longer time for detachment event while retraction. Moreover, it can be seen that for Figure 4.3 (c), force at F for 7 μl (▲) is less than zero, which indicates the larger residual volume on the substrate as the force sensor was calibrated to zero after drop generation. In summary, higher the drop volume, larger the base diameter that further increases the apparent adhesion force experienced by the force sensor. It is worth mentioning that, similar to wettability, irrespective of drop volume or procedure to quantify it, the magnitude of surface energy must remain constant.

Role of compression

In this section, adhesion force profile is studied with the variation of compression. The selected compressions are 0.0, 0.2, and 0.3 mm in air medium for PMMA, Teflon and PA. On the other hand, in water medium, they are 0.0, 0,2, 0.4, and 0.6 mm

for PMMA, Teflon and Cu surfaces as depicted in Figure 4.4. The higher magnitude in compression for liquid medium case is attributed to the drainage of surrounding medium liquid prior to the formation of drop-substrate interface. Due to viscous nature of liquid, compared to air, the additional efforts are required to form the interface hence higher magnitude of compressions are required.
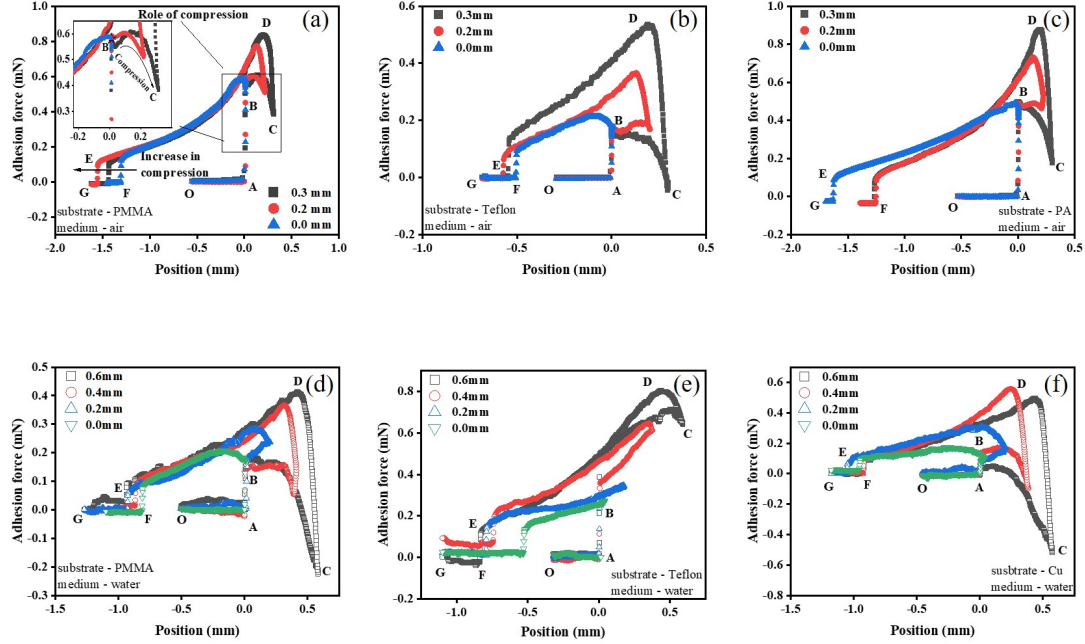
Figure 4.4: Force-distance curve recorded for varying compression value between water droplet and (a) PMMA, (b) Teflon, (c) PA in air medium; whereas between oil droplet (D10) and (d) PMMA, (e) Teflon, (f) Cu in water medium. Here the drop volume is kept approximately 4 μl for all the measurements.

Irrespective of the surrounding medium, the liquid droplet is pushed forcefully against the substrate to achieve complete and equilibrium spreading. Figure 4.4 (a) (enlarged view) shows the slope of the B − C curve is changing and experiences more repulsion between liquid droplet and the substrate as the compression increases from 0.2 mm (●) to 0.3 mm (■). Higher the compression larger the drop base diameter, which resembles the droplet volume scenario explained earlier. Thus, higher the drop volume or compression results in a similar outcome of higher F_{max} for the same solid-liquid-medium combinations. It is important to point out that there is a certain

limit on compression value, after which F_{max} might decrease, even after an increase in compression. This threshold depends on the solid-liquid interface, surrounding medium, and other operating parameters (which will be discussed in the next section with an example).On the other hand, the spreading force (B) remains the same, as the change in compression does not affect the spreading force due to no change in drop volume.

4.4.3 Accurate quantification of adhesion force

To further analyze the total adhesion force experienced by the force sensor, it is also essential to study the effect of the above-mentioned operating parameters on components of adhesion force individually. This aspect provides insights into the significance of TPCL role, which is directly affected by varying operating parameters like drop volume and compression. The components of adhesion force are the surface tension force, acting along the perimeter of TPCL, and the Laplace pressure force, due to the pressure difference across the liquid-gas interface[150, 183], this can be presented as:

$$F_{max} = 2\pi r \gamma \ sin\theta_{ms} - \pi r^2 \ \triangle P \qquad (4.1)$$

Where, F_{max} is the total vertical maximum adhesion force measured at D (Figure 4.1 (c and d)), r is the droplet base radius, γ is the surface tension or interfacial tension of probe liquid in the air or liquid medium, respectively, θ_{ms} is the most stable contact angle of the liquid measured with the substrate[173].

$\triangle$ P is the Laplace pressure force:

$$\triangle P = \gamma \left(\frac{1}{D} - \frac{1}{R} \right) \qquad (4.2)$$

where D and R are the principal radii of the spreading or adhered water droplet as it can be seen in Figure 4.1 (b).

Clearly, from the equation 4.1, surface tension force ($F_{s,max}$) and Laplace pressure force ($F_{L,max}$), measured at F_{max} are the function of TPCL, recognized as droplet base radius (r) in the equation, which is a dependent variable of drop volume and compression. Hence, variation in any of the operating parameters will directly affect these two force components and consequently the total adhesion force.
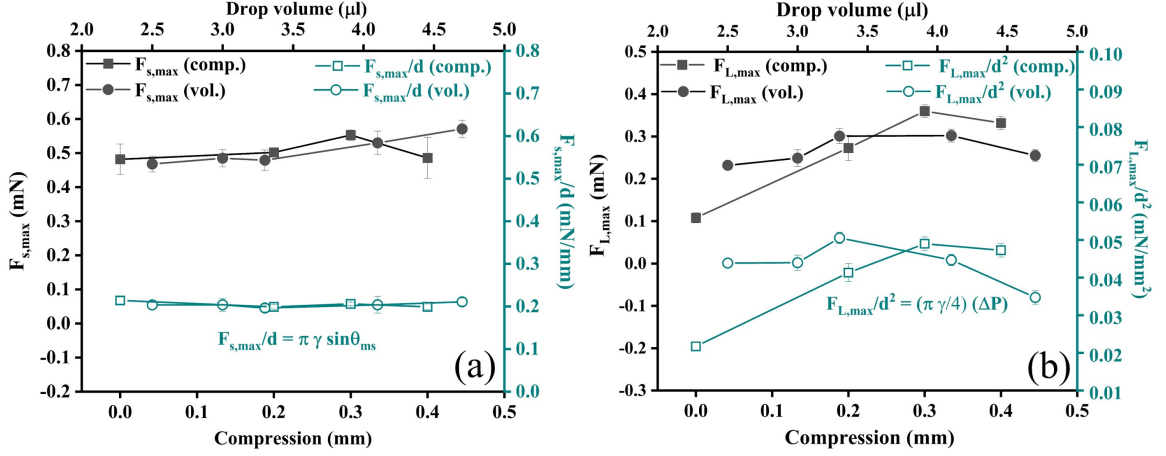
Figure 4.5: Shows (a) surface tension force ($F_{s,max}$) and (b) Laplace pressure force ($F_{L,max}$) at F_{max} for PMMA surface with water droplet in air medium, vary with drop volume and compression. Also, both the components are divided with their corresponding power of base diameter from the equation.

Figure 4.5 shows the influence of change in drop volume and compression on $F_{s,max}$ and $F_{L,max}$ individually. From Figure 4.5 (a), it is evident that $F_{s,max}$ for drop volume increases linearly; however, with compression, it increases first until 0.3 mm compression and then decreases. On the other hand, in Figure 4.5 (b), $F_{L,max}$ increases along with the increase in drop volume until ∼ 4 µl and then decreases due to increase in radii of curvature. Moreover, $F_{L,max}$ with compression shows similar behavior as $F_{s,max}$, increasing till 0.3 mm and then decreasing. The possible explanation for this trend would be as compression increases from 0.3 mm to 0.4 mm, the base diameter measured at F_{max} decreases (see Table 4.2), resulting in a reduction in surface tension force, and Laplace pressure force. Conclusively, a similar trend is also observed for the total adhesion force (F_{max}) with compression, as shown in Figure 4.6. It is noted
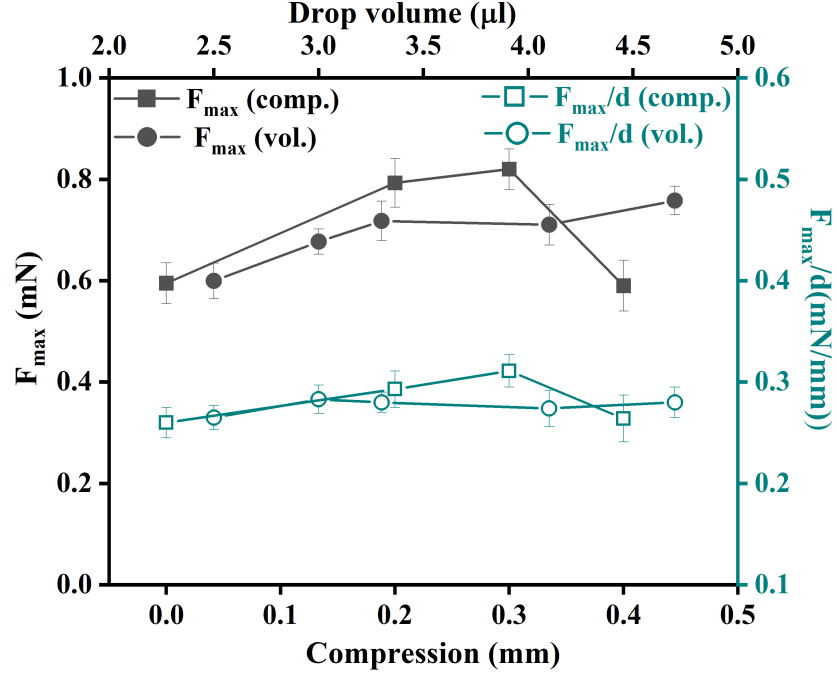
Figure 4.6: Shows maximum adhesion force (F_{max}) and F_{max} per unit length varies with drop volume and compression for PMMA surface with water droplet in air medium.

that F_{max} (Figure 4.6) is the experimentally recorded total vertical adhesion force by the force sensor. Furthermore, for the drop volume case, it is observed that the variation in F_{max} is the resultant of surface tension force and Laplace pressure force.

To remove the possible influence of the operating parameters on the adhesion force magnitude, each force is normalized with respect to their power of droplet base diameter (d). $F_{s,max}$ and $F_{L,max}$ are normalized with d and d^2, respectively (Figure 4.5). Also, F_{max} is normalized with its corresponding d, as shown in Figure 4.6. After normalizing, $F_{s,max}$ becomes independent of operating parameters and depends only on the function of $sin\theta_{ms}$, which remains constant with compression and drop volume. However, in the case of $F_{L,max}$, the trend of the curve has not changed, even after the normalization. This can be attributed to the dominance of $\triangle P$ over d^2 in $F_{L,max}$. To support this, if we observe F_{max} per unit length, variation can be seen, especially with compression. Although $F_{s,max}$ per unit length is independent of the compression pa-

rameter, F_{max} per unit length does not show the same conduct. Hence, it would be an incorrect judgment to normalize the total adhesion force with droplet base diameter only, assuming that the surface tension force is the dominant force. Therefore, it is important to notice that not only surface tension is the dominant contributing force, but also Laplace pressure substantially contributes to determine the total adhesion force.

Table 4.2: Shows experimental ($F_{max(exp)}$) and calculated ($F_{max(calc.)}$) maximum adhesion force for PMMA surface with water droplet in air medium with different magnitude of compression.

Comp. (mm)	d (mm)	θ_{ms} (°)	$F_{s,max}$ (mN)	$F_{L,max}$ (mN)	$F_{max(calc.)}$ (mN)	$F_{max(exp)}$ (mN)	Variation %
	± 0.33	± 3.67	± 0.05	± 0.08	± 0.13	± 0.09	
0.4	2.48	62.12	0.45	-0.23	0.64	0.59	8.4
0.3	2.71	64.44	0.55	-0.36	0.86	0.82	4.9
0.2	2.55	60.63	0.51	-0.27	0.75	0.79	5
0.0	2.29	71.00	0.48	-0.11	0.55	0.59	6.8

Finally, Table 4.2 summarises the total adhesion force calculated by the summation of these two components and compared with the total adhesion force recorded experimentally. Calculated and experimental total adhesion force for water droplet and PMMA in air medium for given conditions are in good agreement.

4.5 Conclusions

This study measures the adhesion force for PMMA, Teflon, and PA with water droplets in an air medium, as well as for PMMA, Teflon and Cu with D10 oil droplets in a water medium using a force tensiometer. The complete measurement process

comprises various stages such as approaching, spreading, compression, retraction, and detachment of the droplet. All these steps were continuously and simultaneously captured using a high-speed CCD camera. Moreover, the influence of different operating parameters like drop volume, compression, and surrounding medium were studied and the following are the concluding remarks.

- It is observed that these operating parameters have a direct impact on F_{max}. The results show the variation in drop volume changes the spreading and F_{max} forces, while compression does not affect the spreading force but the F_{max}.

- Similar results are observed for liquid medium. Whereas, the presence of additional forces such as buoyancy and static pressure influence force magnitude recorded by force tensiometer. Both of these forces need to be subtracted to obtain absolute interactive forces between a liquid droplet and a solid surface. A complete step by step guideline is provided.

- This study also demonstrated that the surface tension force becomes independent of operating parameters once normalized with the base diameter. However, Laplace pressure force still shows variation with these parameters, even after normalizing with base diameter, that shows the importance of Laplace pressure to the total force experienced by the force sensor. Therefore, it is essential to consider both these components while measuring the adhesion force using a force tensiometer for a given solid-liquid interface.

Chapter 5

Conclusions and Future work

5.1 Overview and Summary

As already noted that various authors have been modifying surface textures for a wide variety of applications such as self-cleaning surfaces [4], droplet microfluidics [165], oil-water separation [184], anti-acing surfaces [147] and many more. Adhesion force measurements using a force tensiometer is a highly efficient and easy to use measurement method to characterize surface wettability of such surfaces. The primary objective of this thesis is to address the concerns and overlooked issues related to the measurement of the adhesion force using a micro-electronic mechanical balance system (force tensiometer). We subsequently provide guidelines to measure the accurate and reliable force measurement. Primarily, we focused on the ignored operating parameters that significantly alters the measured adhesion force. Following is the overview and summary of all the topics covered in this project.

Chapter 2 summarizes the literature review of the measurement methods studied for recording surface forces. Derjaguin and Abricossova [96, 98] were the first who measured surface forces experimentally between two solid surfaces using a force-feedback technique in 1954. Inspired by their work, Tabor and Winterton [90] measured forces between two mica surfaces using an optical interference method. Their findings led to the invention of Surface Force Apparatuses (SFAs) in 1972 by Israelachivili and Tabor [104, 109]. The first version of SFA has some limitations, such

as difficulty in cleaning and assembling and unable to determine the spring deflection precisely for low adhesion force. Later, modified versions of the apparatus were able to eliminate previous issues keeping the working principle unchanged. Subsequently, in the late 1980s, the development of the Atomic Force Microscopy (AFM) by G. Binning and C.F. Quate [113] enabled the measurement of surface force interactions of remarkable force sensitivities. More importantly, it served the dual purpose of scanning the surface and measuring the interactive forces simultaneously. Later, other measurement techniques such as droplet probe AFM, scanning droplet adhesion microscopy and many others were also discussed to study the interactive forces between solid-liquid interface. One of the recent techniques which is widely used in characterizing surfaces is adhesion force measurements using a force tensiometer. Conclusively, this literature review narrows down to the examination of common practices/procedures used to record solid-liquid interactions using a tensiometer.

In Chapter 3, a protocol was developed to accurately record the adhesion force between a liquid droplet and a solid surface in air and liquid medium. This protocol starts with the discussion of experimental setup, placement of tensiometer in the laboratory, basic guidelines on optical setup, characterizing surface preparation, drop generation process, and the step by step instructions for force measurement procedure. To analyze the role of the drop holder while forming the solid-liquid interface, the drop generation process and configuration of three different holders namely rod holder, ring holder, and plate holder were investigated. The complete process of measurement of adhesion force consists of several necessary steps such as approaching the substrate towards the droplet, formation of the solid-liquid interface, forceful spreading, retraction, and drop detachment. Complete guidelines were suggested to perform all these steps for both air and liquid medium. Additionally, a separate procedure was also discussed to obtain accurate adhesion force in the liquid medium. It is to be noted that water was used as the surrounding medium. Subsequently,

83

post-measurement approaches were discussed to analyze the obtained data, recorded by force sensor and camera, to achieve the quantified information of force-distance curve, contact angle, and three-phase contact line.

After establishing the guidelines for adhesion force measurements, the influence of different operating parameters, for example, retracting speed, compression, drop volume, and surrounding medium on the adhesion force curve were scrutinized in Chapter 4. Different adhesion force profiles were recorded for a variety of substrates in air and liquid medium with the variation in drop volume and compression. While compression of 0.4 mm is being fixed, drop volume was varied from the range of 2.5 µl to 9 µl to record different force-distance curves. On the other hand, while compression was varied, drop volume was fixed, and Chapter 3 covers the detailed procedure to obtain constant or varying drop volume. It is observed that both parameters have a direct impact on the measured adhesion force in both surrounding mediums (air and liquid). Change in drop volume affects spreading force and maximum adhesion force (F_{max}). As the drop volume increases, the spreading and F_{max} increase monotonically. On the other hand, variation in compression, does not affect the spreading force, but the (F_{max}). In due course, to study the variation in adhesion force or droplet base diameter (d), different components of adhesion force were analyzed, individually. Surface tension and Laplace pressure force were studied with the variation in drop volume and compression. Conclusively, it is observed that surface tension force becomes independent of operating parameters after normalizing with respect to droplet base diameter. However, Laplace pressure force shows variations with both, drop volume and compression, even after normalization with base diameter. In the summary, it is essential to consider both these force components, Laplace pressure and surface tension while measuring the adhesion force using a force tensiometer.

To summarize and contribute the thesis project to the wetting and adhesion com-

munity as follows:

- Describing the existing limitations with the procedure to record interactive forces between a liquid droplet and a solid surface in air or liquid medium.

- The effect of configuration and material properties of drop holder on the force recorded by force sensor was considered and analyzed.

- Establishing an accurate and precise procedure to measure adhesion forces in air medium using a force tensiometer.

- Addressing the additional forces due to liquid medium and proposing the step-wise guidelines to absolutely achieve correct adhesion force with a liquid medium.

- Demonstrating the influence of commonly operating parameters on adhesion force curve in air and liquid medium and investigating the contribution of components of adhesion force, after eliminating the role of droplet base diameter.

5.2 Challenges

The primary concern for an experimental study is to obtain the repeatable and reproducible (R & R) results, hence, measurements in this study were performed atleast five times to incorporate both the errors, instrumentation, and experimentation. To ensure the repeatability and reproducibility of the experiments, there are some observations and important key factors that need to be noticed. To maintain consistency with obtain results, the cleaning of the material substrate should follow the same steps for every experiment. To ensure the cleaning process, it is suggested to measure the surface energy of the substrate initially, using the goniometer before performing adhesion force-based measurements. After cleaning, substrates like Teflon or PMMA get electrostatically charged and can attract the liquid droplet from a far distance

and interferes in the initialization of the experiment. This could be solved by neutralizing the charges present at the solid surface by using the ionizer. Secondly, the major challenge was to generate the oil droplet inside the water due to the overflow of oil through tubings after disconnecting it with the syringe pump. Following, it is important that the substrates and the sample stage must be perfectly flat and horizontal. This is crucial because the force sensor measures net vertical force and small inclination of the substrate or sample stage may record incorrect adhesion force. Finally, it is important to understand that a force tensiometer is a highly sensitive device, hence measuring adhesion force for a low energy solid-liquid interface might be difficult or it can add noise/fluctuations to the force curve.

5.3 Future recommendations

This thesis focuses on precisely measuring the adhesion force in air and liquid medium using a force tensiometer. The investigation of analyzing different operating parameters and their effect on adhesion force curve provides numerous opportunities to obtain any desired wetting results between a liquid and a solid interface. This finding has paved the way for some future captivating studies, which are mentioned as follows:

This study can be further extended in details to maximize the liquid transfer [185, 186] from one solid surface to another for applications like electrophotographic printing [60]. McCarthy and Gao [18, 25, 187–190] have studied the important of contact line over the contact area, which hasn't been quantified experimentally yet. For future work, adhesion force-based measurements could be used as a promising tool to study the contact line dynamics and to justify the role of contact line on wettability gradient surfaces. This can be achieved by obtaining a wettability contrast at the three phase contact line. Adhesion force can be recorded for different thickness of circular ring using chemical surface treatment.

Moreover, recently anisotropic slippery lubricant-infused porous surfaces (SLIPS) [191–194] with the capability of anisotropic self-cleaning [195, 196], self-healing [197], and omniphobic properties [198] have developed and used in the directional transportation of liquids [199] and in reducing ice adhesion [200]. To characterize such surfaces, adhesion force measurements would be an additional performance indicator and would be a major contributing factor to the wetting science community.

On the other hand, as an alternative to modify surface textures at micro or nano scale, electrowetting is a powerful tool used to manipulate liquid droplets sitting on the surface by applying voltage [201–203]. This technique can easily be employed with a force tensiometer, and simultaneously adhesion force would be recorded during droplet deformation in the presence of an electric double layer (EDL).

Bibliography

[1] F. Hizal, N. Rungraeng, J. Lee, S. Jun, H. J. Busscher, H. C. van der Mei, and C.-H. Choi, "Nanoengineered superhydrophobic surfaces of aluminum with extremely low bacterial adhesivity," *ACS applied materials & interfaces*, vol. 9, no. 13, pp. 12 118–12 129, 2017.

[2] T. T. Isimjan, T. Wang, and S. Rohani, "A novel method to prepare superhydrophobic, uv resistance and anti-corrosion steel surface," *Chemical engineering journal*, vol. 210, pp. 182–187, 2012.

[3] C. Jeong, J. Lee, K. Sheppard, and C.-H. Choi, "Air-impregnated nanoporous anodic aluminum oxide layers for enhancing the corrosion resistance of aluminum," *Langmuir*, vol. 31, no. 40, pp. 11 040–11 050, 2015.

[4] K. M. Wisdom, J. A. Watson, X. Qu, F. Liu, G. S. Watson, and C.-H. Chen, "Self-cleaning of superhydrophobic surfaces by self-propelled jumping condensate," *Proceedings of the National Academy of Sciences*, vol. 110, no. 20, pp. 7992–7997, 2013.

[5] X. Zhou, Z. Zhang, X. Xu, F. Guo, X. Zhu, X. Men, and B. Ge, "Robust and durable superhydrophobic cotton fabrics for oil/water separation," *ACS applied materials & interfaces*, vol. 5, no. 15, pp. 7208–7214, 2013.

[6] H. Eral, D. t Mannetje, and J. M. Oh, "Contact angle hysteresis: A review of fundamentals and applications," *Colloid and polymer science*, vol. 291, no. 2, pp. 247–260, 2013.

[7] L. Wen, Y. Tian, and L. Jiang, "Bioinspired super-wettability from fundamental research to practical applications," *Angewandte Chemie International Edition*, vol. 54, no. 11, pp. 3387–3399, 2015.

[8] J. Drelich and A. Marmur, "Physics and applications of superhydrophobic and superhydrophilic surfaces and coatings," *Surface Innovations*, vol. 2, no. 4, pp. 211–227, 2014.

[9] S. Li, J. Huang, Z. Chen, G. Chen, and Y. Lai, "A review on special wettability textiles: Theoretical models, fabrication technologies and multifunctional applications," *Journal of Materials Chemistry A*, vol. 5, no. 1, pp. 31–55, 2017.

[10] W. Barthlott and C. Neinhuis, "Purity of the sacred lotus, or escape from contamination in biological surfaces," *Planta*, vol. 202, no. 1, pp. 1–8, 1997.

[11]   S. L. Sanjay, B. G. Annaso, S. M. Chavan, and S. V. Rajiv, "Recent progress in preparation of superhydrophobic surfaces: A review," *Journal of Surface Engineered Materials and Advanced Technology*, vol. 2012, 2012.

[12]   X.-M. Li, D. Reinhoudt, and M. Crego-Calama, "What do we need for a superhydrophobic surface? a review on the recent progress in the preparation of superhydrophobic surfaces," *Chemical Society Reviews*, vol. 36, no. 8, pp. 1350–1368, 2007.

[13]   G. Zhang, J. Zhang, G. Xie, Z. Liu, and H. Shao, "Cicada wings: A stamp from nature for nanoimprint lithography," *Small*, vol. 2, no. 12, pp. 1440–1443, 2006.

[14]   Y. Jiang and C.-H. Choi, "Droplet retention on superhydrophobic surfaces: A critical review," *Advanced Materials Interfaces*, vol. 8, no. 2, p. 2 001 205, 2021.

[15]   C. Neinhuis and W Barthlott, "Characterization and distribution of water-repellent, self-cleaning plant surfaces," *Annals of botany*, vol. 79, no. 6, pp. 667–677, 1997.

[16]   A. Dupré and P. Dupré, *Théorie mécanique de la chaleur*. Gauthier-Villars, 1869.

[17]   T. Young, "Iii. an essay on the cohesion of fluids," *Philosophical transactions of the royal society of London*, no. 95, pp. 65–87, 1805.

[18]   L. Gao, T. J. McCarthy, and X. Zhang, "Wetting and superhydrophobicity," *Langmuir*, vol. 25, no. 24, pp. 14 100–14 104, 2009.

[19]   B. Bhushan and Y. C. Jung, "Natural and biomimetic artificial surfaces for superhydrophobicity, self-cleaning, low adhesion, and drag reduction," *Progress in Materials Science*, vol. 56, no. 1, pp. 1–108, 2011.

[20]   J. W. Drelich, L. Boinovich, E. Chibowski, C. Della Volpe, L. Hołysz, A. Marmur, and S. Siboni, "Contact angles: History of over 200 years of open questions," *Surface Innovations*, vol. 8, no. 1–2, pp. 3–27, 2019.

[21]   R. N. Wenzel, "Resistance of solid surfaces to wetting by water," *Industrial & Engineering Chemistry*, vol. 28, no. 8, pp. 988–994, 1936.

[22]   A. Cassie, "Contact angles," *Discussions of the Faraday society*, vol. 3, pp. 11–16, 1948.

[23]   P. S. Swain and R. Lipowsky, "Contact angles on heterogeneous surfaces: A new look at cassie's and wenzel's laws," *Langmuir*, vol. 14, no. 23, pp. 6772–6780, 1998.

[24]   A. Cassie and S. Baxter, "Wettability of porous surfaces," *Transactions of the Faraday society*, vol. 40, pp. 546–551, 1944.

[25]   L. Gao and T. J. McCarthy, "How wenzel and cassie were wrong," *Langmuir*, vol. 23, no. 7, pp. 3762–3765, 2007.

[26]   R. Tadmor, "Open problems in wetting phenomena: Pinning retention forces," *Langmuir*, 2021.

[27]   H. Y. Erbil, "The debate on the dependence of apparent contact angles on drop contact area or three-phase contact line: A review," *Surface Science Reports*, vol. 69, no. 4, pp. 325–365, 2014.

[28]   G. Wolansky and A. Marmur, "Apparent contact angles on rough surfaces: The wenzel equation revisited," *Colloids and Surfaces A: Physicochemical and Engineering Aspects*, vol. 156, no. 1-3, pp. 381–388, 1999.

[29]   A. Marmur, "Solid-surface characterization by wetting," *Annual Review of materials research*, vol. 39, pp. 473–489, 2009.

[30]   J. W. Drelich, L. Boinovich, E. Chibowski, C. Della Volpe, L. Hołysz, A. Marmur, and S. Siboni, "Contact angles: History of over 200 years of open questions," *Surface Innovations*, vol. 8, no. 1–2, pp. 3–27, 2019.

[31]   A. Marmur, "Soft contact: Measurement and interpretation of contact angles," *Soft Matter*, vol. 2, no. 1, pp. 12–17, 2006.

[32]   B. Pethica, "Contact angles," *Rep. Prog. Appl. Chem*, vol. 46, pp. 14–17, 1961.

[33]   R. Johnson Jr and R. Dettre, "Surface and colloid science," *Vol. II, E. Matejevic ed., Wiley-Interscience*, pp. 140–42, 1969.

[34]   B. Pethica, "The contact angle equilibrium.," 1977.

[35]   A. Marmur, "A guide to the equilibrium contact angles maze," *Contact angle wettability and adhesion*, vol. 6, no. 3, 2009.

[36]   T. S. Meiron, A. Marmur, and I. S. Saguy, "Contact angle measurement on rough surfaces," *Journal of colloid and interface science*, vol. 274, no. 2, pp. 637–644, 2004.

[37]   A. Marmur, "Thermodynamic aspects of contact angle hysteresis," *Advances in colloid and interface science*, vol. 50, pp. 121–141, 1994.

[38]   T. Huhtamäki, X. Tian, J. T. Korhonen, and R. H. Ras, "Surface-wetting characterization using contact-angle measurements," *Nature protocols*, vol. 13, no. 7, pp. 1521–1538, 2018.

[39]   K. L. Mittal, *Contact Angle, Wettability and Adhesion, Volume 3*. CRC Press, 2003.

[40]   K.-Y. Law and H. Zhao, *Surface wetting: characterization, contact angle, and fundamentals*. Springer International Publishing Basel, Switzerland, 2016.

[41]   B. Samuel, H. Zhao, and K.-Y. Law, "Study of wetting and adhesion interactions between water and various polymer and superhydrophobic surfaces," *The Journal of Physical Chemistry C*, vol. 115, no. 30, pp. 14 852–14 861, 2011.

[42]   H.-J. Butt and M. Kappl, "Normal capillary forces," *Advances in colloid and interface science*, vol. 146, no. 1-2, pp. 48–60, 2009.

[43]   D. Pilat, P Papadopoulos, D Schaffel, D. Vollmer, R. Berger, and H.-J. Butt, "Dynamic measurement of the force required to move a liquid drop on a solid surface," *Langmuir*, vol. 28, no. 49, pp. 16 812–16 820, 2012.

[44] M. Jin, X. Feng, J. Xi, J. Zhai, K. Cho, L. Feng, and L. Jiang, "Super-hydrophobic pdms surface with ultra-low adhesive force," *Macromolecular rapid communications*, vol. 26, no. 22, pp. 1805–1809, 2005.

[45] E Pierce, F. Carmona, and A Amirfazli, "Understanding of sliding and contact angle results in tilted plate experiments," *Colloids and Surfaces A: Physico-chemical and Engineering Aspects*, vol. 323, no. 1-3, pp. 73–82, 2008.

[46] D. Bonn, J. Eggers, J. Indekeu, J. Meunier, and E. Rolley, "Wetting and spreading," *Reviews of modern physics*, vol. 81, no. 2, p. 739, 2009.

[47] M. Cao and L. Jiang, "Superwettability integration: Concepts, design and applications," *Surface Innovations*, vol. 4, no. 4, pp. 180–194, 2016.

[48] K. L. Mittal, *Adhesion measurement of films and coatings*. CRC Press, 2014.

[49] L. B. Boinovich, A. M. Emelyanenko, V. K. Ivanov, and A. S. Pashinin, "Durable icephobic coating for stainless steel," *ACS applied materials & interfaces*, vol. 5, no. 7, pp. 2549–2554, 2013.

[50] N. Gao, F. Geyer, D. W. Pilat, S. Wooh, D. Vollmer, H.-J. Butt, and R. Berger, "How drops start sliding over solid surfaces," *Nature Physics*, vol. 14, no. 2, pp. 191–196, 2018.

[51] B. Bhushan, Y. C. Jung, and K. Koch, "Micro-, nano-and hierarchical structures for superhydrophobicity, self-cleaning and low adhesion," *Philosophical Transactions of the Royal Society A: Mathematical, Physical and Engineering Sciences*, vol. 367, no. 1894, pp. 1631–1672, 2009.

[52] X. Hu, Z. Wang, D. J. Hwang, and T. Cubaud, "Forced wetting and dewetting of water and oil droplets on planar microfluidic grids," *Langmuir*, vol. 36, no. 31, pp. 9269–9275, 2020.

[53] M. Jin, X. Feng, L. Feng, T. Sun, J. Zhai, T. Li, and L. Jiang, "Superhydrophobic aligned polystyrene nanotube films with high adhesive force," *Advanced Materials*, vol. 17, no. 16, pp. 1977–1981, 2005.

[54] K. F. Wiedenheft, H. A. Guo, X. Qu, J. B. Boreyko, F. Liu, K. Zhang, F. Eid, A. Choudhury, Z. Li, and C.-H. Chen, "Hotspot cooling with jumping-drop vapor chambers," *Applied Physics Letters*, vol. 110, no. 14, p. 141 601, 2017.

[55] N. Miljkovic, R. Enright, and E. N. Wang, "Effect of droplet morphology on growth dynamics and heat transfer during condensation on superhydrophobic nanostructured surfaces," *ACS nano*, vol. 6, no. 2, pp. 1776–1785, 2012.

[56] L. Cao, A. K. Jones, V. K. Sikka, J. Wu, and D. Gao, "Anti-icing superhydrophobic coatings," *Langmuir*, vol. 25, no. 21, pp. 12 444–12 448, 2009.

[57] K.-C. Park, H. J. Choi, C.-H. Chang, R. E. Cohen, G. H. McKinley, and G. Barbastathis, "Nanotextured silica surfaces with robust superhydrophobicity and omnidirectional broadband supertransmissivity," *ACS nano*, vol. 6, no. 5, pp. 3789–3799, 2012.

[58] P. Arenkov, A. Kukhtin, A. Gemmell, S. Voloshchuk, V. Chupeeva, and A. Mirzabekov, "Protein microchips: Use for immunoassay and enzymatic reactions," *Analytical biochemistry*, vol. 278, no. 2, pp. 123–131, 2000.

[59] C.-C. Hsieh and S.-C. Yao, "Evaporative heat transfer characteristics of a water spray on micro-structured silicon surfaces," *International Journal of Heat and Mass Transfer*, vol. 49, no. 5-6, pp. 962–974, 2006.

[60] L. B. Schein, *Electrophotography and development physics*. Springer Science & Business Media, 2013, vol. 14.

[61] R. Li, N. Ashgriz, S. Chandra, J. Andrews, and S. Drappel, "Deposition of molten ink droplets on a solid surface," *Journal of Imaging Science and Technology*, vol. 52, no. 2, pp. 20 502–1, 2008.

[62] Y. Son, C. Kim, D. H. Yang, and D. J. Ahn, "Spreading of an inkjet droplet on a solid surface with a controlled contact angle at low weber and reynolds numbers," *Langmuir*, vol. 24, no. 6, pp. 2900–2907, 2008.

[63] H. Zhao and K.-Y. Law, "Super toner and ink repellent superoleophobic surface," *ACS applied materials & interfaces*, vol. 4, no. 8, pp. 4288–4295, 2012.

[64] J Laskowski, "Particle-bubble attachment in flotation," 1974.

[65] P Somasundaran and L Zhang, "Adsorption of surfactants on minerals for wettability control in improved oil recovery processes," *Journal of petroleum science and engineering*, vol. 52, no. 1-4, pp. 198–212, 2006.

[66] N. R. Morrow, "Wettability and its effect on oil recovery," *Journal of petroleum technology*, vol. 42, no. 12, pp. 1476–1484, 1990.

[67] M. Nosonovsky and B. Bhushan, "Superhydrophobic surfaces and emerging applications: Non-adhesion, energy, green engineering," *Current Opinion in Colloid & Interface Science*, vol. 14, no. 4, pp. 270–280, 2009.

[68] Y. Sun, Y. Jiang, C.-H. Choi, G. Xie, Q. Liu, and J. W. Drelich, "Direct measurements of adhesion forces of water droplets on smooth and patterned polymers," *Surface Innovations*, vol. 6, no. 1–2, pp. 93–105, 2017.

[69] U. U. Ghosh, S. Nair, A. Das, R. Mukherjee, and S. DasGupta, "Replicating and resolving wetting and adhesion characteristics of a rose petal," *Colloids and Surfaces A: Physicochemical and Engineering Aspects*, vol. 561, pp. 9–17, 2019.

[70] T. Darmanin, G. Godeau, and F. Guittard, "Superhydrophobic, superoleophobic and underwater superoleophobic conducting polymer films," *Surface Innovations*, vol. 6, no. 4–5, pp. 181–204, 2018.

[71] J. Wang, S. Liu, and S. Guo, "Calcium ions enhanced mussel-inspired underwater superoleophobic coating with superior mechanical stability and hot water repellence for efficient oil/water separation," *Applied Surface Science*, vol. 503, p. 144 180, 2020.

[72] L.-P. Xu, B. Dai, J. Fan, Y. Wen, X. Zhang, and S. Wang, "Capillary-driven spontaneous oil/water separation by superwettable twines," *Nanoscale*, vol. 7, no. 31, pp. 13 164–13 167, 2015.

[73] J. Beyer, H. C. Trannum, T. Bakke, P. V. Hodson, and T. K. Collier, "Environmental effects of the deepwater horizon oil spill: A review," *Marine pollution bulletin*, vol. 110, no. 1, pp. 28–51, 2016.

[74] J. Wang and H. Wang, "Easily enlarged and coating-free underwater superoleophobic fabric for oil/water and emulsion separation via a facile naclo2 treatment," *Separation and Purification Technology*, vol. 195, pp. 358–366, 2018.

[75] H. Zhu, P. Guo, Z. Shang, X. Yu, and Y. Zhang, "Fabrication of underwater superoleophobic metallic fiber felts for oil-water separation," *Applied Surface Science*, vol. 447, pp. 72–77, 2018.

[76] J. Wang and H. Wang, "Integrated device based on cauliflower-like nickel hydroxide particles–coated fabrics with inverse wettability for highly efficient oil/hot alkaline water separation," *Journal of colloid and interface science*, vol. 534, pp. 228–238, 2019.

[77] F. Zhang, W. B. Zhang, Z. Shi, D. Wang, J. Jin, and L. Jiang, "Nanowire-haired inorganic membranes with superhydrophilicity and underwater ultralow adhesive superoleophobicity for high-efficiency oil/water separation," *Advanced Materials*, vol. 25, no. 30, pp. 4192–4198, 2013.

[78] X. Liu, J. Gao, Z. Xue, L. Chen, L. Lin, L. Jiang, and S. Wang, "Bioinspired oil strider floating at the oil/water interface supported by huge superoleophobic force," *ACS nano*, vol. 6, no. 6, pp. 5614–5620, 2012.

[79] M. Jin, S. Li, J. Wang, Z. Xue, M. Liao, and S. Wang, "Underwater superoleophilicity to superoleophobicity: Role of trapped air," *Chemical Communications*, vol. 48, no. 96, pp. 11 745–11 747, 2012.

[80] Q. Zhu, Q. Pan, and F. Liu, "Facile removal and collection of oils from water surfaces through superhydrophobic and superoleophilic sponges," *The Journal of Physical Chemistry C*, vol. 115, no. 35, pp. 17 464–17 470, 2011.

[81] M. Liu, S. Wang, Z. Wei, Y. Song, and L. Jiang, "Bioinspired design of a superoleophobic and low adhesive water/solid interface," *Advanced Materials*, vol. 21, no. 6, pp. 665–669, 2009.

[82] L.-P. Xu, J. Peng, Y. Liu, Y. Wen, X. Zhang, L. Jiang, and S. Wang, "Nacre-inspired design of mechanical stable coating with underwater superoleophobicity," *ACS nano*, vol. 7, no. 6, pp. 5077–5083, 2013.

[83] E. Zhang, Z. Cheng, T. Lv, L. Li, and Y. Liu, "The design of underwater superoleophobic ni/nio microstructures with tunable oil adhesion," *Nanoscale*, vol. 7, no. 45, pp. 19 293–19 299, 2015.

[173] J. W. Drelich, L. Boinovich, E. Chibowski, C. Della Volpe, L. Hołysz, A. Marmur, and S. Siboni, "Contact angles: History of over 200 years of open questions," *Surface Innovations*, vol. 8, no. 1–2, pp. 3–27, 2019.

[163] T. Guo, M. Li, L. Heng, and L. Jiang, "Design of honeycomb structure surfaces with controllable oil adhesion underwater," *RSC advances*, vol. 5, no. 76, pp. 62 078–62 083, 2015.

[84] D. Wang, Y. Jiang, Z. Zhu, W. Yin, K. Asawa, C.-H. Choi, and J. W. Drelich, "Contact line and adhesion force of droplets on concentric ring-textured hydrophobic surfaces," *Langmuir*, vol. 36, no. 10, pp. 2622–2628, 2020.

[85] R. Winterton, "Van der waals forces," *Contemporary Physics*, vol. 11, no. 6, pp. 559–574, 1970.

[86] J. Van der Waals, "On the continuity of the gases and liquid state," *Doctoral Dissertation, Leiden University*, 1873.

[87] I. E. Dzyaloshinskii, E. M. Lifshitz, and L. P. Pitaevskii, "The general theory of van der waals forces," *Advances in Physics*, vol. 10, no. 38, pp. 165–209, 1961.

[88] D. Langbein, "Theory of van der waals attraction," *Springer tracts in modern physics*, pp. 1–139, 1974.

[89] H Margenau, "Van der waals forces," *Reviews of Modern Physics*, vol. 11, no. 1, p. 1, 1939.

[90] D. Tabor and R. S. Winterton, "The direct measurement of normal and retarded van der waals forces," *Proceedings of the Royal Society of London. A. Mathematical and Physical Sciences*, vol. 312, no. 1511, pp. 435–450, 1969.

[91] T. Cosgrove, *Colloid science: principles, methods and applications*. John Wiley & Sons, 2010.

[92] H.-J. Butt, K. Graf, and M. Kappl, *Physics and chemistry of interfaces*. John Wiley & Sons, 2013.

[93] H.-J. Butt, B. Cappella, and M. Kappl, "Force measurements with the atomic force microscope: Technique, interpretation and applications," *Surface science reports*, vol. 59, no. 1-6, pp. 1–152, 2005.

[94] B. V. Derjaguin, N. V. Churaev, V. M. Muller, and V. Kisin, *Surface forces*. Springer, 1987.

[95] J. Kitchener, A. Prosser, and g. surName, "Direct measurement of the long-range van der waals forces," *Proceedings of the Royal Society of London. Series A. Mathematical and Physical Sciences*, vol. 242, no. 1230, pp. 403–409, 1957.

[96] B. Derjaguin, I. Abrikosova, and E. Lifshitz, "Direct measurement of molecular attraction between solids separated by a narrow gap," *Quarterly Reviews, Chemical Society*, vol. 10, no. 3, pp. 295–329, 1956.

[97] P. M. Claesson, T Ederth, V Bergeron, and M. Rutland, "Techniques for measuring surface forces," *Advances in colloid and interface science*, vol. 67, pp. 119–183, 1996.

[98] B. Derjaguin, I. Abrikosova, and E. Lifshitz, "Direct measurement of molecular attraction between solids separated by a narrow gap," *Progress in Surface Science*, vol. 40, no. 1-4, pp. 77–82, 1992.

[99] K. L. Johnson, K. Kendall, and a. Roberts, "Surface energy and the contact of elastic solids," *Proceedings of the royal society of London. A. mathematical and physical sciences*, vol. 324, no. 1558, pp. 301–313, 1971.

[100] A. Pizzi and K. L. Mittal, *Handbook of adhesive technology*. CRC press, 2017.

[101] B. Bhushan, J. N. Israelachvili, and U. Landman, "Nanotribology: Friction, wear and lubrication at the atomic scale," *Nature*, vol. 374, no. 6523, pp. 607–616, 1995.

[102] D Tabor, "Surface forces and surface interactions," in *Plenary and invited lectures*, Elsevier, 1977, pp. 3–14.

[103] K. Fuller and D. Tabor, "The effect of surface roughness on the adhesion of elastic solids," *Proceedings of the Royal Society of London. A. Mathematical and Physical Sciences*, vol. 345, no. 1642, pp. 327–342, 1975.

[104] J. N. Israelachvili and D. Tabor, "The measurement of van der waals dispersion forces in the range 1.5 to 130 nm," *Proceedings of the Royal Society of London. A. Mathematical and Physical Sciences*, vol. 331, no. 1584, pp. 19–38, 1972.

[105] J. Israelachvili, *Direct measurements of forces between surfaces in liquids at the molecular level*, 1987.

[106] J. N. Israelachvili and G. Adams, "Direct measurement of long range forces between two mica surfaces in aqueous kno3 solutions," *Nature*, vol. 262, no. 5571, pp. 774–776, 1976.

[107] J. N. Israelachvili, *Intermolecular and surface forces*. Academic press, 2011.

[108] R. G. Horn and J. N. Israelachvili, "Direct measurement of structural forces between two surfaces in a nonpolar liquid," *The Journal of Chemical Physics*, vol. 75, no. 3, pp. 1400–1411, 1981.

[109] J. N. Israelachvili and G. E. Adams, "Measurement of forces between two mica surfaces in aqueous electrolyte solutions in the range 0–100 nm," *Journal of the Chemical Society, Faraday Transactions 1: Physical Chemistry in Condensed Phases*, vol. 74, pp. 975–1001, 1978.

[110] L. R. Fisher and J. N. Israelachvili, "Direct measurement of the effect of meniscus forces on adhesion: A study of the applicability of macroscopic thermodynamics to microscopic liquid interfaces," *Colloids and Surfaces*, vol. 3, no. 4, pp. 303–319, 1981.

[111] V. S. Craig, "An historical review of surface force measurement techniques," *Colloids and Surfaces A: Physicochemical and Engineering Aspects*, vol. 129, pp. 75–93, 1997.

[112] J. N. Israelachvili and P. M. McGuiggan, "Adhesion and short-range forces between surfaces. part i: New apparatus for surface force measurements," *Journal of Materials Research*, vol. 5, no. 10, pp. 2223–2231, 1990.

[113] C. Gerber, C. Quate, and G Binning, "Atomic force microscope," *Phys. Rev. Lett*, vol. 56, pp. 930–933, 1986.

[114] R. Garcıa and R. Perez, "Dynamic atomic force microscopy methods," *Surface science reports*, vol. 47, no. 6-8, pp. 197–301, 2002.

[115] J. Chen, *Introduction to Scanning Tunneling Microscopy Third Edition*. Oxford University Press, USA, 2021, vol. 69.

[116] C. Rotsch and M. Radmacher, "Mapping local electrostatic forces with the atomic force microscope," *Langmuir*, vol. 13, no. 10, pp. 2825–2832, 1997.

[117] Y. Martin, C. C. Williams, and H. K. Wickramasinghe, "Atomic force microscope–force mapping and profiling on a sub 100-Å scale," *Journal of applied Physics*, vol. 61, no. 10, pp. 4723–4729, 1987.

[118] M. Kappl and H.-J. Butt, "The colloidal probe technique and its application to adhesion force measurements," *Particle & Particle Systems Characterization: Measurement and Description of Particle Properties and Behavior in Powders and Other Disperse Systems*, vol. 19, no. 3, pp. 129–143, 2002.

[119] Y. F. Dufrêne, D. Martínez-Martín, I. Medalsy, D. Alsteens, and D. J. Müller, "Multiparametric imaging of biological systems by force-distance curve–based afm," *Nature methods*, vol. 10, no. 9, pp. 847–854, 2013.

[120] W. A. Ducker, T. J. Senden, and R. M. Pashley, "Direct measurement of colloidal forces using an atomic force microscope," *Nature*, vol. 353, no. 6341, pp. 239–241, 1991.

[121] S Maghsoudy-Louyeh, M Kropf, and B. Tittmann, "Review of progress in atomic force microscopy," *The Open Neuroimaging Journal*, vol. 12, no. 1, 2018.

[122] F. J. Giessibl, "Advances in atomic force microscopy," *Reviews of modern physics*, vol. 75, no. 3, p. 949, 2003.

[123] B. Cappella and G. Dietler, "Force-distance curves by atomic force microscopy," *Surface science reports*, vol. 34, no. 1-3, pp. 1–104, 1999.

[124] A. Weisenhorn, P Maivald, H.-J. Butt, and P. Hansma, "Measuring adhesion, attraction, and repulsion between surfaces in liquids with an atomic-force microscope," *Physical Review B*, vol. 45, no. 19, p. 11 226, 1992.

[125] H.-J. Butt and M. Kappl, *Surface and interfacial forces*. John Wiley & Sons, 2018.

[126] D. Daniel, Y. Florida, C. L. Lay, X. Q. Koh, A. Sng, and N. Tomczak, "Quantifying surface wetting properties using droplet probe atomic force microscopy," *ACS Applied Materials & Interfaces*, vol. 12, no. 37, pp. 42 386–42 392, 2020.

[127] V. Liimatainen, M. Vuckovac, V. Jokinen, V. Sariola, M. J. Hokkanen, Q. Zhou, and R. H. Ras, "Mapping microscale wetting variations on biological and synthetic water-repellent surfaces," *Nature communications*, vol. 8, no. 1, pp. 1–7, 2017.

[128] P. M. Brakefield, J. Gates, D. Keys, F. Kesbeke, P. J. Wijngaarden, A. Montelro, V. French, and S. B. Carroll, "Development, plasticity and evolution of butterfly eyespot patterns," *Nature*, vol. 384, no. 6606, pp. 236–242, 1996.

[129] N. J. Nadeau, C. Pardo-Diaz, A. Whibley, M. A. Supple, S. V. Saenko, R. W. Wallbank, G. C. Wu, L. Maroja, L. Ferguson, J. J. Hanly, *et al.*, "The gene cortex controls mimicry and crypsis in butterflies and moths," *Nature*, vol. 534, no. 7605, pp. 106–110, 2016.

[130] D. A. Olsen, P. A. Joyner, and M. D. Olson, "The sliding of liquid drops on solid surfaces," *The Journal of Physical Chemistry*, vol. 66, no. 5, pp. 883–886, 1962.

[131] C. Antonini, F. Carmona, E Pierce, M Marengo, and A Amirfazli, "General methodology for evaluating the adhesion force of drops and bubbles on solid surfaces," *Langmuir*, vol. 25, no. 11, pp. 6143–6154, 2009.

[132] R. Tadmor, P. Bahadur, A. Leh, H. E. N'guessan, R. Jaini, and L. Dang, "Measurement of lateral adhesion forces at the interface between a liquid drop and a substrate," *Physical review letters*, vol. 103, no. 26, p. 266 101, 2009.

[133] H.-J. Butt, I. V. Roisman, M. Brinkmann, P. Papadopoulos, D. Vollmer, and C. Semprebon, "Characterization of super liquid-repellent surfaces," *Current opinion in colloid & interface science*, vol. 19, no. 4, pp. 343–354, 2014.

[134] E. Beach, G. Tormoen, J Drelich, and R Han, "Pull-off force measurements between rough surfaces by atomic force microscopy," *Journal of Colloid and Interface Science*, vol. 247, no. 1, pp. 84–99, 2002.

[135] J. Liu, B. Yu, B. Ma, X. Song, X. Cao, Z. Li, W. Yang, and F. Zhou, "Adhesion force spectroscopy of model surfaces with wettability gradient," *Colloids and Surfaces A: Physicochemical and Engineering Aspects*, vol. 380, no. 1-3, pp. 175–181, 2011.

[136] P. Rios, H Dodiuk, and S Kenig, "Self-cleaning coatings," *Surface engineering*, vol. 25, no. 2, pp. 89–92, 2009.

[137] F. L. Geyer, E. Ueda, U. Liebel, N. Grau, and P. A. Levkin, "Superhydrophobic–superhydrophilic micropatterning: Towards genome-on-a-chip cell microarrays," *Angewandte Chemie International Edition*, vol. 50, no. 36, pp. 8424–8427, 2011.

[138] Z. Xue, S. Wang, L. Lin, L. Chen, M. Liu, L. Feng, and L. Jiang, "A novel superhydrophilic and underwater superoleophobic hydrogel-coated mesh for oil/water separation," *Advanced Materials*, vol. 23, no. 37, pp. 4270–4273, 2011.

[139] B. Su, S. Wang, Y. Song, and L. Jiang, "Utilizing superhydrophilic materials to manipulate oil droplets arbitrarily in water," *Soft Matter*, vol. 7, no. 11, pp. 5144–5149, 2011.

[140] H Chen, A Amirfazli, and T Tang, "Modeling liquid bridge between surfaces with contact angle hysteresis," *Langmuir*, vol. 29, no. 10, pp. 3310–3319, 2013.

[141] W. Barthlott and C. Neinhuis, "Purity of the sacred lotus, or escape from contamination in biological surfaces," *Planta*, vol. 202, no. 1, pp. 1–8, 1997.

[142] Y. Jiao, S. Gorb, and M. Scherge, "Adhesion measured on the attachment pads of tettigonia viridissima (orthoptera, insecta)," *Journal of Experimental Biology*, vol. 203, no. 12, pp. 1887–1895, 2000.

[143] K. Koch, B. Bhushan, and W. Barthlott, "Multifunctional surface structures of plants: An inspiration for biomimetics," *Progress in Materials science*, vol. 54, no. 2, pp. 137–178, 2009.

[144] R. Fürstner, W. Barthlott, C. Neinhuis, and P. Walzel, "Wetting and self-cleaning properties of artificial superhydrophobic surfaces," *Langmuir*, vol. 21, no. 3, pp. 956–961, 2005.

[145] A. A. Darhuber, S. M. Troian, and S. Wagner, "Physical mechanisms governing pattern fidelity in microscale offset printing," *Journal of Applied Physics*, vol. 90, no. 7, pp. 3602–3609, 2001.

[146] P. Calvert, "Inkjet printing for materials and devices," *Chemistry of materials*, vol. 13, no. 10, pp. 3299–3305, 2001.

[147] A. Ganne, K. I. Maslakov, and A. I. Gavrilov, "Anti-icing properties of superhydrophobic stainless steel mesh at subzero temperatures," *Surface Innovations*, vol. 5, no. 3, pp. 154–160, 2017.

[148] M. Grüßer, D. G. Waugh, J. Lawrence, N. Langer, and D. Scholz, "On the droplet size and application of wettability analysis for the development of ink and printing substrates," *Langmuir*, vol. 35, no. 38, pp. 12 356–12 365, 2019.

[149] J. Drelich, "Guidelines to measurements of reproducible contact angles using a sessile-drop technique," *Surface innovations*, vol. 1, no. 4, pp. 248–254, 2013.

[150] J. Qian and H. Gao, "Scaling effects of wet adhesion in biological attachment systems," *Acta biomaterialia*, vol. 2, no. 1, pp. 51–58, 2006.

[151] Y. Sun, Y. Jiang, C.-H. Choi, G. Xie, Q. Liu, and J. W. Drelich, "The most stable state of a droplet on anisotropic patterns: Support for a missing link," *Surface Innovations*, vol. 6, no. 3, pp. 133–140, 2018.

[152] Y. Sun, Y. Li, X. Dong, X. Bu, and J. W. Drelich, "Spreading and adhesion forces for water droplets on methylated glass surfaces," *Colloids and Surfaces A: Physicochemical and Engineering Aspects*, vol. 591, p. 124 562, 2020.

[153] R. Lacombe, *Adhesion Measurements methods:theory and practice*, 1st Edition. 2005, ISBN: 9780429114168. DOI: https://doi-org.login.ezproxy.library.ualberta.ca/10.1201/9781420028829.

[154] D. Daniel, C. L. Lay, A. Sng, C. J. J. Lee, D. C. J. Neo, X. Y. Ling, and N. Tomczak, "Mapping micrometer-scale wetting properties of superhydrophobic surfaces," *Proceedings of the National Academy of Sciences*, vol. 116, no. 50, pp. 25 008–25 012, 2019.

[155] M. Eriksson and A. Swerin, "Forces at superhydrophobic and superamphiphobic surfaces," *Current Opinion in Colloid & Interface Science*, vol. 47, pp. 46–57, 2020.

[156] H Chen, T Tang, H Zhao, K.-Y. Law, and A Amirfazli, "How pinning and contact angle hysteresis govern quasi-static liquid drop transfer," *Soft Matter*, vol. 12, no. 7, pp. 1998–2008, 2016.

[157] H Chen, T Tang, and A Amirfazli, "Liquid transfer mechanism between two surfaces and the role of contact angles," *Soft matter*, vol. 10, no. 15, pp. 2503–2507, 2014.

[158] P. R. Waghmare, N. S. K. Gunda, and S. K. Mitra, "Under-water superoleophobicity of fish scales," *Scientific reports*, vol. 4, no. 1, pp. 1–5, 2014.

[159] Q. Cheng, M. Li, Y. Zheng, B. Su, S. Wang, and L. Jiang, "Janus interface materials: Superhydrophobic air/solid interface and superoleophobic water/solid interface inspired by a lotus leaf," *Soft Matter*, vol. 7, no. 13, pp. 5948–5951, 2011.

[160] S Nishimoto and B Bhushan, *Bioinspired self-cleaning surfaces with superhydrophobicity, superoleophobicity, and superhydrophilicity. rsc adv 3 (3): 671–690*, 2013.

[161] L. Zhang, Z. Zhang, and P. Wang, "Smart surfaces with switchable superoleophilicity and superoleophobicity in aqueous media: Toward controllable oil/water separation," *NPG Asia Materials*, vol. 4, no. 2, e8–e8, 2012.

[162] W. Liu, X. Liu, J. Fangteng, S. Wang, L. Fang, H. Shen, S. Xiang, H. Sun, and B. Yang, "Bioinspired polyethylene terephthalate nanocone arrays with underwater superoleophobicity and anti-bioadhesion properties," *Nanoscale*, vol. 6, no. 22, pp. 13 845–13 853, 2014.

[164] J. Y. Huang, Y.-C. Lo, J. J. Niu, A. Kushima, X. Qian, L. Zhong, S. X. Mao, and J. Li, "Nanowire liquid pumps," *Nature nanotechnology*, vol. 8, no. 4, pp. 277–281, 2013.

[165] I. Shestopalov, J. D. Tice, and R. F. Ismagilov, "Multi-step synthesis of nanoparticles performed on millisecond time scale in a microfluidic droplet-based system," *Lab on a Chip*, vol. 4, no. 4, pp. 316–321, 2004.

[166] M. A. Sarshar, C. Swarctz, S. Hunter, J. Simpson, and C.-H. Choi, "Effects of contact angle hysteresis on ice adhesion and growth on superhydrophobic surfaces under dynamic flow conditions," *Colloid and Polymer Science*, vol. 291, no. 2, pp. 427–435, 2013.

[167] M. Ma and R. M. Hill, "Superhydrophobic surfaces," *Current opinion in colloid & interface science*, vol. 11, no. 4, pp. 193–202, 2006.

[168] C.-H. Choi and C.-J. Kim, "Large slip of aqueous liquid flow over a nano-engineered superhydrophobic surface," *Physical review letters*, vol. 96, no. 6, p. 066 001, 2006.

[169] B Pignataro, A Licciardello, S Cataldo, and G. Marletta, "Spm and tof-sims investigation of the physical and chemical modification induced by tip writing of self-assembled monolayers," *Materials Science and Engineering: C*, vol. 23, no. 1-2, pp. 7–12, 2003.

[170] H Hantsche, "Comparison of basic principles of the surface-specific analytical methods: Aes/sam, esca (xps), sims, and iss with x-ray microanalysis, and some applications in research and industry," *Scanning*, vol. 11, no. 6, pp. 257–280, 1989.

[171] V. I. Silin, H. Wieder, J. T. Woodward, G. Valincius, A Offenhausser, and A. L. Plant, "The role of surface free energy on the formation of hybrid bi-layer membranes," *Journal of the American Chemical Society*, vol. 124, no. 49, pp. 14 676–14 683, 2002.

[172] A.-A. Dhirani, R. W. Zehner, R. P. Hsung, P. Guyot-Sionnest, and L. R. Sita, "Self-assembly of conjugated molecular rods: A high-resolution stm study," *Journal of the American Chemical Society*, vol. 118, no. 13, pp. 3319–3320, 1996.

[174] G. Binnig, C. F. Quate, and C. Gerber, "Atomic force microscope," *Physical review letters*, vol. 56, no. 9, p. 930, 1986.

[175] J. N. Israelachvili, "Adhesion forces between surfaces in liquids and condensable vapours," *Surface Science Reports*, vol. 14, no. 3, pp. 109–159, 1992.

[176] J. Wong, A. Chilkoti, and V. T. Moy, "Direct force measurements of the streptavidin–biotin interaction," *Biomolecular engineering*, vol. 16, no. 1-4, pp. 45–55, 1999.

[177] J Israelachvili, Y Min, M Akbulut, A Alig, G Carver, W Greene, K Kristiansen, E Meyer, N Pesika, K Rosenberg, *et al.*, "Recent advances in the surface forces apparatus (sfa) technique," *Reports on Progress in Physics*, vol. 73, no. 3, p. 036 601, 2010.

[178] V. J. Morris, A. R. Kirby, and P. A. Gunning, *Atomic force microscopy for biologists*. World Scientific, 2009.

[179] B Cappella, P Baschieri, C Frediani, P Miccoli, and C Ascoli, "Force-distance curves by afm," *IEEE engineering in medicine and biology magazine*, vol. 16, no. 2, pp. 58–65, 1997.

[180] M. Liu, Y. Zheng, J. Zhai, and L. Jiang, "Bioinspired super-antiwetting interfaces with special liquid- solid adhesion," *Accounts of chemical research*, vol. 43, no. 3, pp. 368–377, 2010.

[181] Q. Cheng, M. Li, F. Yang, M. Liu, L. Li, S. Wang, and L. Jiang, "An underwater ph-responsive superoleophobic surface with reversibly switchable oil-adhesion," *Soft Matter*, vol. 8, no. 25, pp. 6740–6743, 2012.

[182] K.-Y. Law, *Definitions for hydrophilicity, hydrophobicity, and superhydrophobicity: Getting the basics right*, 2014.

[183] F. Orr, L. Scriven, and A. P. Rivas, "Pendular rings between solids: Meniscus properties and capillary force," *Journal of Fluid Mechanics*, vol. 67, no. 4, pp. 723–742, 1975.

[184] H. Gao, Y. Liu, G. Wang, S. Li, Z. Han, and L. Ren, "Switchable wettability surface with chemical stability and antifouling properties for controllable oil–water separation," *Langmuir*, vol. 35, no. 13, pp. 4498–4508, 2019.

[185] H.-c. Huang and N. S. Zacharia, "Layer-by-layer rose petal mimic surface with oleophilicity and underwater oleophobicity," *Langmuir*, vol. 31, no. 2, pp. 714–720, 2015.

[186] H Chen, T Tang, and A Amirfazli, "Effects of surface wettability on fast liquid transfer," *Physics of Fluids*, vol. 27, no. 11, p. 112 102, 2015.

[187] L. Gao and T. J. McCarthy, "Contact angle hysteresis explained," *Langmuir*, vol. 22, no. 14, pp. 6234–6237, 2006.

[188] L. Gao and T. J. McCarthy, "An attempt to correct the faulty intuition perpetuated by the wenzel and cassie "laws"," *Langmuir*, vol. 25, no. 13, pp. 7249–7255, 2009.

[189] D. F. Cheng and T. J. McCarthy, "Using the fact that wetting is contact line dependent," *Langmuir*, vol. 27, no. 7, pp. 3693–3697, 2011.

[190] S. F. Chini, V Bertola, and A Amirfazli, "A methodology to determine the adhesion force of arbitrarily shaped drops with convex contact lines," *Colloids and Surfaces A: Physicochemical and Engineering Aspects*, vol. 436, pp. 425–433, 2013.

[191] Z. Xiao, Q. Zhao, Y. Niu, and D. Zhao, "Adhesion advances: From nanomaterials to biomimetic adhesion and applications," *Soft Matter*, vol. 18, no. 18, pp. 3447–3464, 2022.

[192] J. Wang, L. Wang, N. Sun, R. Tierney, H. Li, M. Corsetti, L. Williams, P. K. Wong, and T.-S. Wong, "Viscoelastic solid-repellent coatings for extreme water saving and global sanitation," *Nature Sustainability*, vol. 2, no. 12, pp. 1097–1105, 2019.

[193] M. Tenjimbayashi, R. Togasawa, K. Manabe, T. Matsubayashi, T. Moriya, M. Komine, and S. Shiratori, "Liquid-infused smooth coating with transparency, super-durability, and extraordinary hydrophobicity," *Advanced Functional Materials*, vol. 26, no. 37, pp. 6693–6702, 2016.

[194] R. Togasawa, M. Tenjimbayashi, T. Matsubayashi, T. Moriya, K. Manabe, and S. Shiratori, "A fluorine-free slippery surface with hot water repellency and improved stability against boiling," *ACS applied materials & interfaces*, vol. 10, no. 4, pp. 4198–4205, 2018.

[195] X. Meng, Z. Wang, L. Wang, L. Heng, and L. Jiang, "A stable solid slippery surface with thermally assisted self-healing ability," *Journal of Materials Chemistry A*, vol. 6, no. 34, pp. 16 355–16 360, 2018.

[196] L. Wang and T. J. McCarthy, "Covalently attached liquids: Instant omniphobic surfaces with unprecedented repellency," *Angewandte Chemie International Edition*, vol. 55, no. 1, pp. 244–248, 2016.

[197] Z. Wang, L. Heng, and L. Jiang, "Effect of lubricant viscosity on the self-healing properties and electrically driven sliding of droplets on anisotropic slippery surfaces," *Journal of Materials Chemistry A*, vol. 6, no. 8, pp. 3414–3421, 2018.

[198] T.-S. Wong, S. H. Kang, S. K. Tang, E. J. Smythe, B. D. Hatton, A. Grinthal, and J. Aizenberg, "Bioinspired self-repairing slippery surfaces with pressure-stable omniphobicity," *Nature*, vol. 477, no. 7365, pp. 443–447, 2011.

[199] X. Wang, Z. Wang, L. Heng, and L. Jiang, "Stable omniphobic anisotropic covalently grafted slippery surfaces for directional transportation of drops and bubbles," *Advanced Functional Materials*, vol. 30, no. 1, p. 1 902 686, 2020.

[200] S. B. Subramanyam, K. Rykaczewski, and K. K. Varanasi, "Ice adhesion on lubricant-impregnated textured surfaces," *Langmuir*, vol. 29, no. 44, pp. 13 414–13 418, 2013.

[201] L. Joly, C. Ybert, E. Trizac, and L. Bocquet, "Hydrodynamics within the electric double layer on slipping surfaces," *Physical review letters*, vol. 93, no. 25, p. 257 805, 2004.

[202] Y.-P. Zhao and Q. Yuan, "Statics and dynamics of electrowetting on pillar-arrayed surfaces at the nanoscale," *Nanoscale*, vol. 7, no. 6, pp. 2561–2567, 2015.

[203] X. He, W. Qiang, C. Du, Q. Shao, X. Zhang, and Y. Deng, "Modification of lubricant infused porous surface for low-voltage reversible electrowetting," *Journal of Materials Chemistry A*, vol. 5, no. 36, pp. 19 159–19 167, 2017.